

SARATR-X: A Foundation Model for Synthetic Aperture Radar Images Target Recognition

Weijie Li, Wei Yang*, Yuenan Hou, Li Liu*, Yongxiang Liu*, Xiang Li

Abstract—Synthetic aperture radar (SAR) is essential in actively acquiring information for Earth observation. SAR Automatic Target Recognition (ATR) focuses on detecting and classifying various target categories under different image conditions. The current deep learning-based SAR ATR methods are typically designed for specific datasets and applications. Various target characteristics, scene background information, and sensor parameters across ATR datasets challenge the generalization of those methods. This paper aims to achieve general SAR ATR based on a foundation model with Self-Supervised Learning (SSL). Our motivation is to break through the specific dataset and condition limitations and obtain universal perceptual capabilities across the target, scene, and sensor. A foundation model named SARATR-X is proposed with the following four aspects: pre-training dataset, model backbone, SSL, and evaluation task. First, we integrated 14 datasets with various target categories and imaging conditions as a pre-training dataset. Second, different model backbones were discussed to find the most suitable approaches for remote-sensing images. Third, we applied two-stage training and SAR gradient features to ensure the diversity and scalability of SARATR-X. Finally, SARATR-X has achieved competitive and superior performance on 5 datasets with 8 task settings, which shows that the foundation model can achieve universal SAR ATR. We believe it's time to embrace fundamental models for SAR image interpretation in the era of increasing big data.

Index Terms—Synthetic Aperture Radar (SAR), Target Recognition, Foundation Model, Self-Supervised Learning (SSL), Deep Learning, Masked Image Modeling (MIM)

INTRODUCTION

BASED on electromagnetic scattering in microwave frequency bands, Synthetic Aperture Radar (SAR) [22, 53, 62] is essential in actively acquiring information for Earth observation with stable imaging capacity under various weather and lighting conditions. SAR Automatic Target Recognition (ATR) aims to automatically localize and classify interested objects in SAR images, *e.g.*, detection and classification. It has been investigated extensively with various civilian and military applications [36, 57, 69, 73]. In the past decade, deep learning has reinvigorated SAR ATR with impressive breakthroughs [15, 31, 37]. However, as shown in Fig 1 and 2, due to the extensive acquisition conditions as well as the high costs of collection and annotation, there are a plethora of special datasets and algorithms designed for different applications of SAR ATR. For example, nearly a dozen new target datasets and dozens of attention modules have been developed for SAR target recognition in the last few years. However, the target characteristics, scene background information and sensor parameters across datasets challenge their generalization. In contrast to specialized algorithms for particular applications, we aim to investigate *a general SAR target recognition method*.

A foundation model [5] pre-trained in a task-agnostic manner (generally via self-supervision learning) on extensive data can be flexibly adapted to a wide range of downstream tasks under various conditions. Self-supervised learning (SSL) [4,

45] can mitigate label inefficiency by exploring supervision directly from the data itself, thereby reducing reliance on expensive expert labeling and efficiently scaling data and models. Hence, SSL has the capability to leverage extensive SAR unlabeled data for constructing foundational models, which can achieve universal recognition with a few labeled target samples in different categories and conditions. As shown in Table 1, foundation models are thriving in remote sensing with superior performance in a diverse range of modalities and tasks. In particular, multi-modality foundation models have recently appeared, indicating this research topic's great potential. But, there lacks a foundation model that can effectively accomplish various tasks for SAR ATR, such as FG-MAE [79] and SkySense [26] mainly focus on SAR scene classification and segmentation, and our previous SAR-JEPA [38] and MSFA [43] explored the object classification and detection tasks separately. It is still necessary to explore the development of an analogous ATR foundation model for SAR image interpretation, which lies at the intersection of SAR technologies and frontier AI technologies (in particular, the big models).

Thanks to the development of SAR sensors and the enormous efforts of researchers, numerous SAR target datasets have emerged over the past five years in Fig. 2. Despite image annotation remaining a challenging and expensive endeavor, SAR sensors have produced vast amounts of data at a significantly accelerated pace compared to the previous ten years. Meanwhile, the investigation of SSL and foundation models for SAR ATR is advancing with increasing datasets. As shown in Table 1, existing research [38, 43, 56, 79, 92] have discussed different factors of a foundation model, and these studies are progressively advancing towards a goal of achieving general SAR ATR. For example, BIDFC [92] performs much better than supervised methods in the few-shot classification of the MSTAR vehicle dataset, SAR-JEPA [38] demonstrates that SSL can effectively improve the classification accuracy for

*This work was supported by the National Key Research and Development Program of China No. 2021YFB3100800, the National Natural Science Foundation of China under Grant 61871384, 61921001, 62022091, 62201588, and 62376283, the Science and Technology Innovation Program of Hunan Province under Grant 2022RC1092, and the Key Stone Grant JS2023-03 of the National University of Defense Technology. (*Corresponding authors: Li Liu, Wei Yang, and Yongxiang Liu. e-mail: liuli_nudt@nudt.edu.cn, yw850716@sina.com, and lyx_bible@sina.com.)*

Weijie Li, Wei Yang, Yongxiang Liu, Li Liu, Xiang Li are with the College of Electronic Science and Technology, National University of Defense Technology, Changsha, 410073, China (e-mail: lwj2150508321@sina.com).

Yuenan Hou is with the Shanghai AI Laboratory, Shanghai, 200000, China.

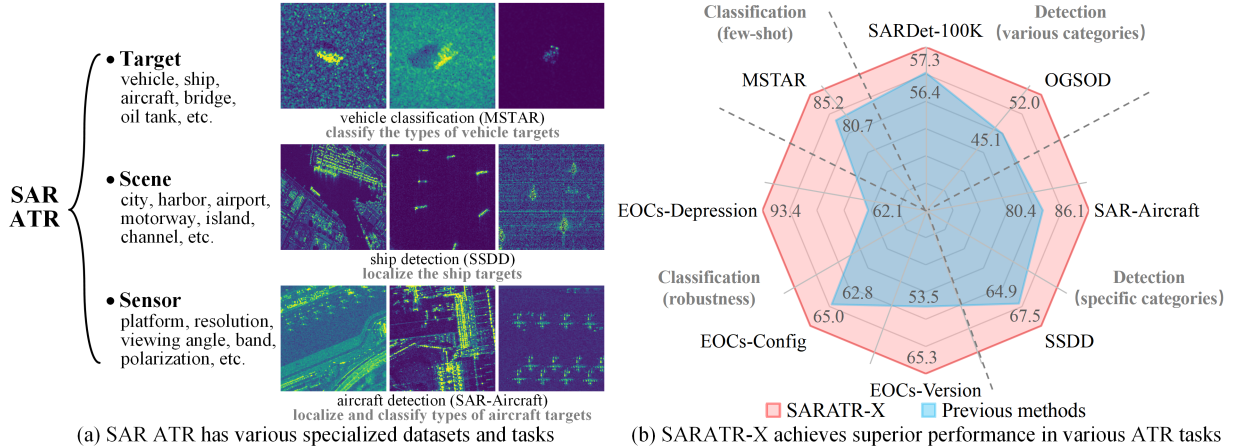


Fig. 1: Motivation and performance of SARATR-X. (a) SAR ATR has various imaging conditions, including targets, scenes, and sensors. However, due to high cost, its datasets are collected under specific settings and tasks. For example, the MSTAR dataset [1] is a ten-type vehicle target classification dataset in X-band and grass scenarios, while SAR-Aircraft is a seven-type aircraft target detection dataset in three airports and a C-band satellite. Many specialized algorithms have been proposed for these datasets. However, the different target characteristics, scene background information and sensor parameters between these datasets challenge the generalization of existing algorithms. This paper aims to explore a SAR ATR foundation model, a general method to achieve various tasks. (b) Our SARATR-X performs well on 5 datasets with 8 settings compared with previous methods. For target classification, SARATR-X is better than the previous SSL method (BIDFC [92]) on fine-grained vehicle MSTAR dataset [1] with the few-shot setting. Besides, it performs well under extended operating conditions (EOCs) [94], *i.e.*, the imaging condition variation in depression angle (EOCs-Depression), target configuration (EOCs-Config), and version (EOCs-Version). For object detection, SARATR-X demonstrates competitive performance with previous carefully designed supervised methods on various categories (SARDet-100K [43] and OGSOD [71]) and specific categories on ship (SSDD [97]), and aircraft (SAR-Aircraft [80]). Our study shows the potential of the foundation model for universal SAR target recognition.

different targets across datasets, and MSFA [43] shows improved results of ship detection. Inspired by their insightful work, we formally propose a SAR ATR foundation model, **SARATR-X**, to achieve a breakthrough in universal SAR target recognition.

In this work, we lay the groundwork for developing SARATR-X, a foundation model specifically tailored for SAR ATR tasks. It aims to learn generalizable representations from unlabeled SAR images, offering a basis for efficient adaptation across various downstream ATR tasks. The four parts for creating SARATR-X include pre-training datasets, model backbones, self-supervised learning, and evaluation tasks.

Pre-training datasets need to contain diverse target categories and imaging conditions to accommodate various downstream tasks. However, SAR ATR lacks a large-scale dataset like ImageNet [19], and the most used MSTAR dataset in Table 2 only includes fine-grained vehicle categories, which is not suitable for larger-scale pre-training. Therefore, many SSL methods combine different datasets; in particular, SARDet-100K incorporates [43] 9 SAR target detection datasets. With the increasing number of open-source datasets for SAR ATR, we integrate the vast majority of them for pre-training. As shown in Fig 2 and Table 3, we apply 14 classification and detection datasets with different target categories and imaging conditions to explore the foundation model’s potential.

Model backbones aim to achieve better spatial representation in remote sensing images, especially small target signatures in large imagery. As shown in Table 1, researchers used two architectures (Transformer or convolutional neural network). Transformer has better spatial resolution without downsampling, and Convolutional Neural Network (CNN) has higher efficiency with its convolution kernel. MSFA discussed the effectiveness of different architectures, and the results showed that the Swin Transformer backbone performs better. Therefore, we discuss different model backbones to find the most

suitable approaches for the properties of remote sensing images. HiViT [99] is our choice, which combines Swin Transformer advantages and can drop patches in MIM.

Self-supervised learning faces the challenge of SAR image quality. SAR images contain speckle noise due to coherent imaging, and their visual features are not as distinct and rich as RGB images. As shown in Table 2, contrastive learning [56, 92] uses data augmentation and pre-processing to reduce noise, while MIM [38, 43, 79] has a pixel-to-feature improvement for guide signals. Therefore, we consider that the problem to be solved by SAR SSL is how to construct high-quality guide signals. For example, PGIL [29] leveraged a sub-frequency feature of SAR complex images to learn physics information, and our SAR-JEPA [38] applied multi-scale gradient ratio to solve multiplicative speckle noise and capture target shape. Furthermore, multi-stage speckle training [43] from ImageNet to SAR diminished noise interference on model diversity in Fig. 5. Therefore, we apply two-stage training from ImageNet to SAR and use multi-scale gradient features as high-quality guide signals for SAR MIM.

Evaluation tasks need to comprehensively evaluate the performance of the foundation model under different tasks and settings. Benefiting from the open-source target datasets, we first construct a fine-grained classification dataset with various categories to evaluate the effectiveness of the proposed improvements. In the end, we perform a comprehensive comparison between the proposed SARATR-X and existing SOTA methods in public classification and detection tasks.

Our SARATR-X has achieved a competitive and superior performance on 5 datasets with 8 task settings in Fig 1. And its codes and weights can be found at <https://github.com/waterdisappear/SARATR-X>. We hope this work will advance the development of foundation models and general SAR target recognition. The main contributions are summarized as follows:

TABLE 1: List of visual foundation models in remote sensing. There are many foundation models for various modalities and tasks, but research (FG-MAE, SkySense, and OFA-Net) focuses on scene-level tasks with the SAR modality. Based on our previous study SAR-JEPA and MSFA [38, 43], SARATR-X fills this gap in the foundation model for SAR ATR. These foundation models’ SSL methods are divided into two approaches: one is contrastive, such as contrastive learning, to obtain invariant features; another is generative, such as masked image modeling, to generate and predict features. SD: Stable Diffusion. Swin: Swin Transformer.

Foundation model	Year	Modality	Dataset	Backbone	SSL	Tasks
SatMAE [13]	2022	Multi-spectral, RGB	fMoW RGB/Sentinel	ViT	Generative	Scene classification and semantic segmentation
RVSA [77]	2022	RGB	MillionAID	ViT, ViTAE	Generative	Scene classification, object detection, and semantic segmentation
RingMo [65]	2022	RGB	Self-built	ViT, Swin	Generative	Scene classification, object detection, semantic segmentation, and change detection
RingMo-Sense [90]	2023	RGB	Self-built	Video Swin	Generative	object detection and tracking, images segmentation, and 3 prediction tasks
CMID [55]	2023	RGB	MillionAID	ResNet, Swin	Generative & Contrastive	Scene classification, object detection, and semantic segmentation
GFM [52]	2023	RGB	GeoPile	Swin	Generative	Scene classification, semantic segmentation, change detection, and super-resolution
DiffusionSat [32]	2023	RGB	fMoW, Satlas, SpaceNet	SD	Generative	Image generation, super-resolution, temporal generation, and in-painting
Scale-MAE [58]	2023	RGB	fMoW RGB	ViT	Generative	Scene classification, object detection, and semantic segmentation
FG-MAE [79]	2023	Multi-spectral, SAR	SSL4EO-S12	ViT	Generative	Scene classification and semantic segmentation
SMLFR [17]	2024	RGB	GeoSense	ConvNeXt	Generative	Object detection, semantic segmentation, and change detection
SkySense [26]	2024	3 modalities	HSROIs, TMsI, TSARI	Swin, Vit	Contrastive	Scene classification, object detection, semantic segmentation, and change detection
OFA-Net [87]	2024	4 modalities	5 multi-modalities datasets	ViT	Generative	Scene Classification and semantic segmentation
SAR-JEPA [38]	2024	SAR	MSAR, SAR-Ship, SARSim, SAMPLE	ViT	Generative	Target classification
MSFA [43]	2024	SAR	ImageNet, DOTA, SARDet-100k	CNN, ViT, Swin	Generative	Object detection
SARATR-X	2024	SAR	ImageNet & 14 SAR datasets	HiViT	Generative	Target classification and object detection

- We propose a vision of general SAR target recognition, aiming to find universal solutions for various SAR ATR tasks and application in an era of SAR images with big unlabeled data and small labeled samples.
- We have systematically investigated a foundation model solution for general SAR ATR and present the first SAR ATR foundation model named SARATR-X, which achieves new performance breakthroughs on a wide range of SAR target recognition datasets and settings.
- We hope this promising work will stimulate research interest in SAR foundation models, thereby advancing SAR image interpretation with frontier AI technologies.

The remainder of this paper is organized as follows. Sec. 2 introduces related work in remote sensing and SAR ATR. Sec. 3 introduces the proposed foundation model SARATR-X. Sec. 4 and 5 conducts extensive experiments to demonstrate the superiority of the proposed method. Sec. 6 concludes the paper and discusses future work.

2 RELATED WORK

As shown in Table 1 and 2, visual foundation models are booming in remote sensing. Many models are proposed for various modalities and tasks. Our studies focus on the foundation model for SAR ATR, *i.e.*, SAR images-based target classification and object detection. In the following, we introduce the recent development of remote sensing foundation models.

2.1 Foundation models in remote sensing

Remote sensing foundation models [30] have received widespread attention in the last three years. Researchers have made many breakthroughs, achieving effective learning on various modalities and tasks. In terms of pre-training datasets, researchers use existing large-scale datasets or collect a large number of samples from different sources. As for the model backbone, researchers have improved attention mechanisms, positional encoding, and other aspects to enhance the perception of complex spatial information. MIM has been used to learn spatial-temporal contextual information, while contrast learning is applied to multi-modal learning.

SatMAE [13] proposed a novel masking strategy and temporal and spectral positional encoding for multi-spectral and temporal images. With a new dataset fMoW Sentinel with 13 frequency bands, SatMAE achieved new performance on scene classification and semantic segmentation tasks. RVSA [77] improved the pretraining ViT backbone with a rotated varied-size window attention method for the arbitrary-oriented objects. This work shows the importance of learning targets’ complex spatial contextual relationships in remote sensing images. RingMo [65] used a patch incomplete mask strategy for dense and small objects. Based on their self-built 2 million images, RingMo has proven effective in many tasks. RingMo-Sense [90] offered a three-branch network and masking strategy to model the spatio-temporal interaction for temporal images. CMID [55] combined contrastive learning and masked image

TABLE 2: Related work about SSL and foundation models for SAR ATR. It can be found that the exploration of the foundation model in SAR ATR. Researchers have explored different dataset settings, CNN and Transformer architectures, and various SSL algorithms. Inspired by their successful work, we formally present the first SAR ATR foundation model, SARATR-X, to achieve various recognition tasks.

Method	Year	Dataset	Backbone	SSL	Tasks	Description
RotANet [82]	2021	MSTAR	CNN	Generative	Target classification (MSTAR)	Predicting rotational patterns of targets as a loss regularization term for classification task.
UACL [88]	2021	MSTAR, FUSAR-Ship	CNN	Contrastive	Target classification (MSTAR)	Contrastive defense method to enhance model robustness to different adversarial attack.
PGIL [29]	2022	sea-ice, urban	ResNet-18	Contrastive	Scene classification (sea-ice, urban)	Contrastive learning between sub-frequency features of complex images and deep features of amplitude images.
BIDFC [92]	2022	MSTAR, OpenSARShip	ResNet-18	Contrastive	Target classification (MSTAR, OpenSARShip)	Weakly contrastive learning for pre-training in fine-grained datasets with similar sample.
TSCL [56]	2023	MSTAR	ResNet-50	Contrastive	Target classification (MSTAR, OpenSARShip)	Pre-processing of SAR images for noise removal to improve image quality for Contrastive learning.
FG-MAE [79]	2023	SSL4EO-S12	ViT-S	Generative	Scene classification (EuroSAT, BigEarthNet-MM), semantic segmentation (DFC2020)	Hand-craft feature HOG as the target signal for MIM in SAR images.
SAR-JEPA [38]	2024	MSAR, SAR-Ship, Sarsim, SAMPLE	ViT-B	Generative	Target classification (MSTAR, FUSARShip, SAR-ACD)	Local reconstruction and multi-scale gradient feature for MIM with small object in noise SAR images.
MSFA [43]	2024	ImageNet, DOTA, SARDet-100k	Swin-B	Generative	Object detection (SARDet-100K, SSDD, HRSID)	Multi-stage pre-training strategy for MIM from RGB images to SAR images.
SARATR-X	2024	ImageNet, 14 SAR target datasets	HiViT-B	Generative	Target classification and Object detection (5 datasets and 8 settings)	A first foundation model for target recognition in SAR Images.

modeling to learn global semantic information and local spatial information. GFM [52] focused on the differences between natural and remote sensing images and employed a multi-objective continual pretraining approach to leverage both knowledge. DiffusionSat [32] was the first remote sensing generative that employs geographic information embedding in stable diffusion. Scale-MAE [58] reconstructed images at different frequencies with improved positional encodings of ViT. FG-MAE [79] employed different hand-designed features to replace the original pixels in the MIM and improve the feature quality. And SMLFR [17] used a low pass filter to eliminate high-frequency information from the image pixel.

Multi-modal remote sensing foundation models have been developed, such as SkySense [26] and OFA-Net [87]. SkySense [26] proposed a multi-granularity contrastive learning method to learn representations of different modalities. Besides, a GEO-context prototype was applied to embed geographical contextual information. OFA-Net [87] applied a shared Transformer backbone for multiple modalities. Besides this, there are vision-language models [41], such as EarthGPT [98], SkyEyeGPT [93] and LHRs-Bot [54], which incorporate large language models to different remote sensing images modalities. However, due to the difficulty of annotating SAR images, the collection of public datasets used by EarthGPT only has 10,554 SAR ship images, much less than 84,838 infrared images and 907,945 optical images.

Therefore, there is relatively less research on SAR foundation models due to the scarcity and fragmentation of the high-resolution SAR target datasets in Fig 2. We want to explore the visual foundation model based on SAR images with target recognition to stimulate research enthusiasm in this direction.

2.2 Foundation models in SAR

Researchers have explored SAR foundation models in different aspects, as shown in Table 2. Inspired by previous studies, we systematically investigated how to construct a SAR ATR foundation model.

Early SSL was often used as a regularization loss for classification tasks. RotANet [82] predicted the rotational pattern of MSTAR vehicle targets to capture azimuthal features for the classification task. UACL [88] combined data augmentation and adversarial samples in contrastive learning to improve the model’s robustness to various adversarial attacks. PGIL [29] used contrastive learning between the SAR complex images’ sub-frequency feature and the amplitude images’ deep feature to inject physical knowledge into the classification task. Recently, SSL has been used in model pre-training and fine-tuning frameworks. BIDFC [92] proposed weakly contrastive learning for pre-training in fine-grained vehicle datasets MSTAR and used Gaussian noise data augmentation to simulate SAR image noise. TSCL [56] applied the pre-processing of SAR images before data augmentation in contrastive learning. FG-MAE [79] discussed different hand-craft features for multi-spectral and SAR images and used the HOG feature for SAR. Our previous study, SAR-JEPA [38] and MSFA [43], focused on target classification and object detection. SAR-JEPA [38] applied Local reconstruction and multi-scale gradient feature to capture target spatial signatures better. MSFA [43] proposed a multi-stage with filter augmentation pre-training framework to use large-scale RGB and SAR data for detection.

Our insight. These studies have demonstrated that SSL can achieve performance improvements on various categories [38] and tasks [38, 43], and can even be comparable to the performance of specially designed supervised methods [43, 92].

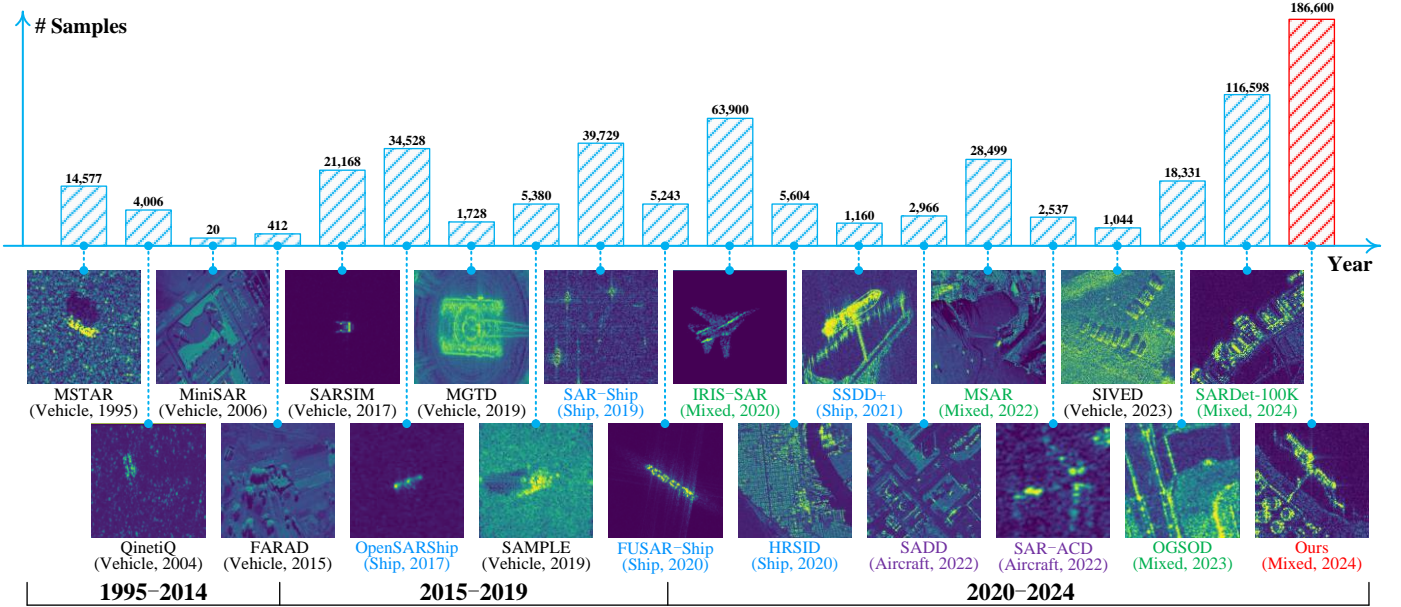


Fig. 2: Timeline of measured and simulated datasets for SAR target recognition (SAR magnitude images were processed in pseudo-color for better visualization). SAR target datasets have increased rapidly since the 2020s, greatly enriching the diversity of targets, scenes, and sensors. Target categories are mainly fine-grained vehicles, ships, and aircraft. Mixed means that the target category includes more than one category, such as a mixture containing various vehicles, ships, and aircraft in IRIS-SAR. Scenes contain cities, harbors, airports, etc. Sensors are devices with different resolutions and bands under satellite or airborne platforms. However, the number of samples (No. samples) in most datasets is only a few thousand with several categories due to the high costs and difficult annotation. It inspired us to propose SARATR-X with an integrated dataset in Table 3.

TABLE 3: Description of our pre-training dataset for SARATR-X, which contains 14 open-source SAR datasets for pre-training. # Img.: Number of images. # Target: Number of target categories. # Scene: Number of scenes. Res.: Resolution. Pol.: Polarization. Large SAR imagery in detection datasets contains more target and scene types than the annotation. We cropped some large images to increase the training samples.

Dataset	Year	# Img.	Img. size	# Target	# Scene	Res. (m)	Band	Pol.	Description
AIR-SARShip [66]	2019	801	512 ~ 1000	≥ 1	≥ 3	1 ~ 3	C	Single	Ship detection dataset in complex scenes
HRSID [81]	2020	5,604	800	≥ 1	≥ 2	0.5 ~ 3	C/X	Quad	Ship detection and instance segmentation dataset
Sandia MiniSAR [60]	2006	3,927	224	≥ 1	≥ 7	0.1	Ku	Single	Terrestrial targets in urban areas, airports, deserts, and others
MSAR [10, 84]	2022	28,499	256 ~ 2048	≥ 4	≥ 6	1	C	Quad	Terrestrial and maritime targets detection dataset
MSTAR [1]	1995	14,577	128 ~ 193	10	1	0.3	X	Single	Fine-grained vehicle classification dataset
OGSOD [71]	2023	18,331	256	≥ 3	≥ 2	3	C	Double	Detection dataset for bridges, oil tanks, and harbours
OpenSARShip [35]	2017	26,679	9 ~ 445	14	10	2.3 ~ 17.4	C	Double	Fine-grained maritime target slices
SADD [96]	2022	883	224	≥ 1	≥ 2	0.5 ~ 3	X	Single	Aircraft detection dataset
SAMPLE [34]	2019	5,380	128	10	2	0.3	X	Single	Simulation and measured vehicle dataset
SAR-Aircraft [80]	2023	18,818	512	≥ 7	≥ 3	1	C	Single	Aircraft detection dataset
SARSim [33, 51]	2017	21,168	139	14	3	0.3	X	Single	Simulation vehicle dataset
SAR-Ship [78]	2019	39,729	256	≥ 1	≥ 4	3 ~ 25	C	Quad	Ship detection dataset in complex scenes
SIVED [44]	2023	1,044	512	≥ 1	≥ 4	0.1 ~ 0.3	X/Ku/Ka	Single	Synthetic vehicle detection dataset
SSDD [97]	2021	1,160	214 ~ 668	≥ 1	≥ 2	1 ~ 15	C/X	Quad	Ship detection dataset

These inspired us to conduct systematic research for foundation models to achieve general SAR target recognition, especially in this era of big data. Firstly, we must extend the pre-dataset with different tasks and scenarios based on existing research. Secondly, a suitable model backbone needs to be discussed for the small target characteristics of remote-sensing images. Thirdly, SSL needs high-quality guide signals from SAR images under noise interference. Finally, we need to evaluate the performance of foundation models comprehensively.

3 APPROACH

We aim to construct a foundation model for general ATR from large-scale SAR images via the SSL method. As described above, the increasing SAR datasets and SSL studies inspired us to build a foundation model for SAR ATR. Our approach revolves around pre-training datasets, model backbones, SSL methods, and evaluation tasks to provide a systematic benchmark for foundation models in SAR ATR.

3.1 Creating a Diverse Pre-training Dataset

Existing work mainly used MSTAR [1] as a pre-training dataset. While MSTAR is a high-quality vehicle target slice dataset, its commonly used samples are only a few thousand. Besides, this dataset suffers from background bias due to a single imaging scene [39]. By comparison, the pre-training set ImageNet-1K in computer vision contains 1.4 million images with different categories and scenes. Using an insufficient SAR target pre-training dataset would underestimate the potential of this research area. Since diverse targets, scenes, and sensor conditions constitute a huge data sampling space in real-world situations, constructing a large pre-training dataset for the foundation model is central to unifying various SAR ATR tasks.

The increasing SAR target datasets in Fig. 2 is a primary motivation for achieving this goal. Although SAR images are expensive and no single dataset contains all popular target categories and various imaging conditions, collecting target samples from various open-source datasets can still construct a pre-training dataset with different categories, scenes,

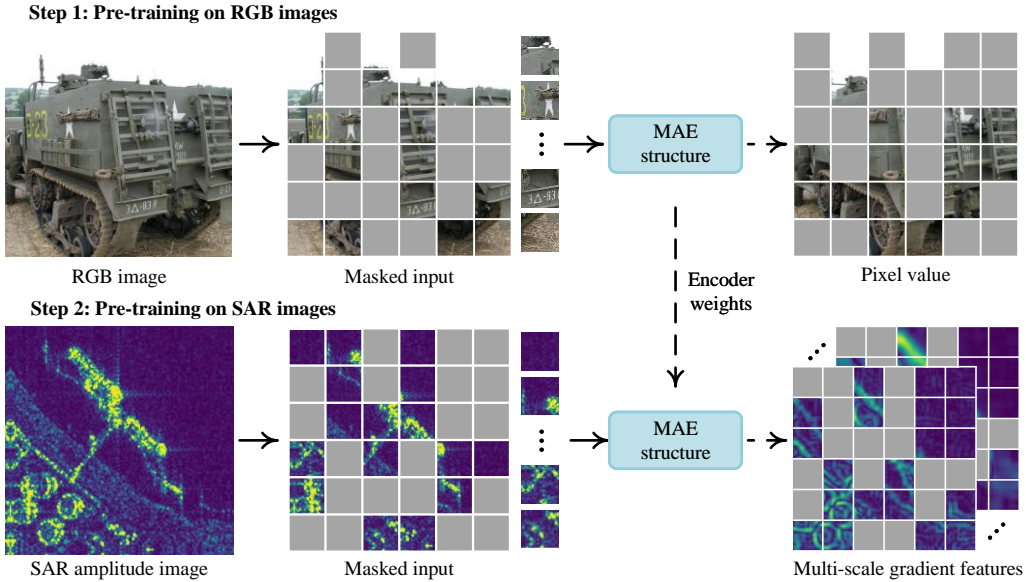


Fig. 3: Two steps of our pre-training. The first is to perform MIM on ImageNet to obtain better initialization weights, as shown in Fig 5 (c). Besides, we can easily obtain the open-source pre-training weights in step 1, thus reducing the pre-training time. The second is to perform MIM on SAR images with high-quality guide signals. We use multi-scale gradient features to suppress speckle noise and extract target edges.

and sensors. Therefore, we build a new pre-training dataset containing 186,600 SAR target samples from 14 open-source SAR target datasets in Table 3. We construct the dataset to include, as much as possible, target categories (terrestrial and maritime targets such as vehicles, ships, aircraft, oil tanks, bridges, etc.), scenes (typical scenes such as cities, harbors, airports, oceans, etc.), and sensors (satellite, airborne, and simulation platforms of different resolutions and bands).

3.2 Choosing a Scalable Model

We consider two model backbones for SAR target recognition. For the first, we apply Vision Transformer (ViT) [18], commonly used in SSL and has good scalability in model parameters. For the second architecture, we experiment with ConvNeXt-V2 [83], which has the same scalability as ViT and maintains the efficiency of convolutional neural networks. In addition to the scalability of the model parameters, the image properties need to be considered for remote sensing. The SAR target usually has a small foreground and a dynamic context range. Our previous study, MSFA [43], finds that the Swin Transformer is better than ViT with a hierarchical structure, but it is unsuitable for drop patches in MIM to save computing resources. Therefore, we also consider a variant of ViT, Hierarchical Vision Transformer (HiVit) [99], which improves the input spatial resolution and retains the property of ViT with MIM.

3.3 Pre-Training with two steps

We use MIM as the pretext task and masked autoencoders (MAE) [27] to save computational resources with dropping patches. MIM can help the foundation model achieve SAR image interpretation by recognizing the contextual relationship around objects. Here is a key point when applying MIM. SAR images belong to coherent imaging, and values have speckle noise that can interfere with the pretext task. Therefore, SARATR-X uses two pre-training steps to build a foundation model in Fig 3.

The first step is to perform MIM on ImageNet to obtain better initialization weights. We simplify the multi-stage pre-training

of MSFA, which performs SSL on ImageNet with backbone, detection task pre-training on DOTA with the whole framework, and detection task fine-tuning on SAR images. SARATR-X uses the pre-training weight of ImageNet as initialization weights for the SAR pre-training step. This way enhances the diversity of attention during the SAR pre-training step in Fig. 5. In contrast, random initialization leads to a convergence of attention towards the same pattern in SAR pre-training with MAE. Besides, ImageNet pre-training backbone weights can be obtained from open source, thus greatly reducing pre-training time. We refer to using ImageNet pre-trained weights as SSL-ImageNet & SAR.

The second step is to perform MIM with SAR images. As mentioned before, SAR image noise is a very tricky problem, and FG-MAR, SAR-JEPA, and MSFA have discussed many features, such as CannyEdge [8], HOG [14], CannyEdge [8], Haar-like [70], SAR-HOG [61] and SAR-SIFT [16]. We can use different feature combinations to get the best results, but here is the simplest gradient feature that follows our previous SAR-JEPA to avoid getting bogged down on complex feature selection. We use the Multi-scale Gradient Feature (MGF) [38] to suppress the speckle noise and extract the target shape.

Multi-scale gradient feature. The classical differential gradient is not a constant false alarm rate operator due to multiplicative speckle noise in the SAR image. It means that speckle noise would cause the gradient computation to have false points in strong target regions. Previous studies [6, 68] have shown that the computing ratio is suitable for multiplicative noise. Here, MGF uses the gradient by ratio [16, 61] to obtain gradient features G_m .

$$R_i = \frac{M_1(i)}{M_2(i)}, \quad (1)$$

$$G_H = \log(R_1), \quad (2)$$

$$G_V = \log(R_3), \quad (3)$$

$$G_m = \sqrt{G_H^2 + G_V^2}, \quad (4)$$

where R_i denotes the average ratio at different directions. $M_1(i)$ and $M_2(i)$ are the area averages on opposite sides of the current

TABLE 4: The results on the classification dataset with 25 categories. We perform the linear probing setting on the few-shot SAR target classification. For the pre-training datasets, we recommend using ImageNet’s pre-trained weights as initialization before pre-training on SAR datasets. For the model backbones, we prefer the HiVit to recognize the small target in SAR images. Model backbones are their base version. The classification metric is average accuracy. **Bold** indicates the best result, underline is the next best result. SL: Supervised Learning. SSL: Self-Supervised Learning.

Backbones	Params	Pre-training			Classification (N-shot)		
		setting	dataset	method	5	10	20
ConvNeXt-V2	89M	SL-ImageNet	ImageNet-1K	Supervised	52.5	61.7	70.5
ConvNeXt-V2	89M	SSL-ImageNet	ImageNet-1K	FCMAE	47.2	54.5	64.0
ConvNeXt-V2	89M	SSL-SAR	SAR images	FCMAE	52.7	60.9	67.7
ConvNeXt-V2	89M	SSL-ImageNet & SAR	ImageNet & SAR	FCMAE	54.7	61.5	69.5
ViT	86M	SL-ImageNet	ImageNet-1K	Supervised	58.6	65.7	74.2
ViT	86M	SSL-ImageNet	ImageNet-1K	MAE	50.7	58.0	65.5
ViT	86M	SSL-SAR	SAR images	MAE	54.1	61.5	68.2
ViT	86M	SSL-ImageNet & SAR	ImageNet & SAR	MAE	65.8	76.4	83.6
HiViT	66M	SL-ImageNet	ImageNet-1K	Supervised	49.0	55.8	63.3
HiViT	66M	SSL-ImageNet	ImageNet-1K	MAE	53.0	60.3	69.3
HiViT	66M	SSL-SAR	SAR images	MAE	64.9	72.7	79.9
<u>HiViT</u>	66M	SSL-ImageNet & SAR	ImageNet & SAR	<u>MAE</u>	<u>71.5</u>	<u>78.5</u>	<u>84.0</u>
HiViT	66M	SSL-ImageNet & SAR	ImageNet & SAR	Ours	76.5	80.8	85.1

pixel along direction i . $i = 1$ is the horizontal direction and $i = 3$ means the vertical direction. The area averages can be computed from the input image and four fixed convolution kernels. Then, Eq. 2 and 3 use logarithms to solve the vertical gradient calculation [16]. G_H is the horizontal gradient and G_V is the vertical gradient.

$$\text{MGF} = \text{concat}(G_{m1}, G_{m2}, G_{m3}) \quad (5)$$

Due to the dynamic range required for various targets in remote sensing [42], MGF is constructed with convolutional kernels of different sizes. We set the kernel scale r equal to 9, 13, and 17 to obtain G_{m1} , G_{m2} , and G_{m3} , and the whole convolutional kernel size is odd square $2r + 1$.

3.4 Evaluating with Recognition Tasks

We merged fine-grained classification datasets of Vehicles, Ships, and Aircraft as a new SAR classification dataset named (SAR-VSA). This dataset is used for comparing the SSL model’s performance with a few-shot setting in Sec. 4. We then report SARATR-X results on existing classification and detection dataset settings with other methods in Sec. 5.

4 EXPERIMENTS OF SARATR-X

First, we perform the SSL on the pre-training dataset without label information. Then, we fine-tune the pre-trained model on SAR-VSA with few-shot classification task and linear probing setting to analyze the improvement of SARATR-X. Finally, we discuss the scalability of the proposed approach.

We perform pre-training on 8 NVIDIA RTX3090 GPUs. The SAR pre-training dataset consists of fourteen SAR datasets. The few-shot SAR classification dataset, SAR-VSA, contains 25 fine-grained targets from the three SAR datasets. It is difficult to ensure training convergence by fine-tuning the model’s whole parameters under small sample cases. Therefore, we use linear probing [27], which includes a batch normalization layer, to adjust the differences in the data statistical properties and reduce the number of fine-tuning parameters. Detailed settings are in the Appendix A.

4.1 Comparison of Model Backbones

Table 4 compares different model backbones for SAR ATR: ConvNeXt-V2 [83], ViT [18], and HiViT [99]. ConvNeXt-V2 and ViT represent the two main architectures: CNN and Transformer. HiViT combines ViT and Swin Transformer [47].

From the result, we can see that ViT outperforms ConvNeXt-V2. On the one hand, the ViT is more flexible than ConvNeXt-V2 in learning the contextual information in SAR images. On the other hand, multiple downsamplings in ConvNeXt-V2 result in the loss of small targets, while ViT maintains the same spatial resolution in different layers. HiViT, a visual Transformer with ViT’s flexibility and hierarchical representation, performs better than ViT and ConvNeXt-V2 in our self-supervised experiments. In particular, HiViT uses small (4×4) input patches, capturing small target features well. Fig. 5 demonstrates that HiViT has a better various attention distance than ViT due to the small target information in remote sensing.

4.2 Strategy of two-step pre-training

Here, we discuss the two-step pre-training strategy to make full use of the available model weights and SAR datasets. Table 4 has four pre-training settings: SL-ImageNet, SSL-ImageNet, SSL-SAR, and SSL-ImageNet & SAR. SL-ImageNet is pre-training on ImageNet with supervised learning¹; SSL-ImageNet is pre-training on ImageNet with SSL from scratch; SSL-SAR is pre-training on our SAR pre-training dataset from scratch; SSL-ImageNet & SAR pre-training the model on SAR dataset based on the initialized weight from SSL-ImageNet.

It is noticed that the additional supervised information introduced by SL-ImageNet does not necessarily improve the SAR ATR performance, *e.g.*, the linear probing performance of SL-ImageNet for HiViT is lower than that of SSL-ImageNet. SSL-SAR can achieve better results than SSL-ImageNet using less data (12%), reflecting the huge differences in the target features between these two images. However, ImageNet pre-training weights can provide a good initialization for low features such as shape and texture in SSL with visible spectral remote

1. We used open-source weights from GitHub to conduct the experiments. The supervised weights of ConvNeXt-V2 and HiViT were obtained by supervised fine-tuning after SSL.

TABLE 5: Comparisons of different target features for MIM. We found many target features are unsuitable for the multiplicative speckle noise in SAR images. This result inspired us to discuss different gradient features for SAR SSL. The pre-training setting SSL-SAR and the model backbones are the base version. The classification metric is average accuracy. **Bold** indicates the best result, underline is the next best result.

Model	Target feature	Classification (N-shot)		
		5	10	20
ViT	pixel value [27]	54.1	61.5	68.2
ViT	low pass filter [46]	53.8	60.5	66.7
ViT	HOG feature [79]	39.7	48.7	56.6
ViT	deep feature [2]	27.8	35.6	41.7
HiViT	pixel value [27]	64.9	72.7	79.9
HiViT	HOG feature [79]	58.2	64.8	71.7
HiViT	<u>SAR-HOG [61]</u>	<u>75.1</u>	<u>80.2</u>	<u>83.9</u>
HiViT	MGF	76.0	81.1	84.5

sensing [67] and medical image [103]. Our experiments also confirmed this conclusion: using SSL-ImageNet as initialization weights improves the pre-training performance of SAR images in Table 4 and attention diversity in Fig. 5. Therefore, our SARATR-X uses the SSL-ImageNet & SAR setting to complement the richness of the pre-training.

4.3 Design of target signal for SAR images

After discussing the backbone and strategy, we focus on the target features for SSL methods with SAR images. Due to the unique multiplicative speckle noise in SAR images, a key point for MIM is designing high-quality guide signals. As shown in Table 5, we consider five target features (pixel value [27], low pass filter [46], HOG feature [79], deep feature [2], SAR-HOG [61], and gradient by ratio [16, 61]). All SSL methods use the SSL-SAR setting and base version.

First, we consider whether the existing methods based on the ViT are suitable for SAR images. PixMIM [46] applies the low pass filter to remove the high-frequency components and drives the model to focus on shape information. However, PixMIM does not outperform MAE because the noise type of SAR is multiplicative, and the filter parameters require a trade-off between target and noise. Then, FG-MAE [79] uses HOG to capture the feature for the SSL with SAR scene-level tasks, but we find that HOG does not ensure high-quality SAR target features. Target regions usually have strong scattering values, and the speckle noise causes the gradient computation to have strong false points in these regions. Besides, I-JEPA [2] propose deep networks as target feature encoders to capture the deep semantic features but lead to training overfitting noise and failure to learn effective feature representations.

Therefore, we choose the SAR features as target features to enhance HiViT. SAR-HOG changes the gradient calculation of HOG features and uses the gradient by ratio to solve speckle noise, and its result performs better than pixel value and HOG. Inspired by PixMIM, we prefer to use the target shape (*i.e.*, gradient features) directly as the target feature ². Besides, multi-scale can improve the feature representation for various small targets in remote sensing. We discuss kernel settings for computing gradient in Fig. 4. Scale can affect feature quality: a smaller scale is finer for small target edge extraction, while a larger scale is more suitable for large target and noise

2. SAR-HOG uses the same multi-scale setting to illustrate that simple gradient features can effectively represent target shape as an SSL guide signal

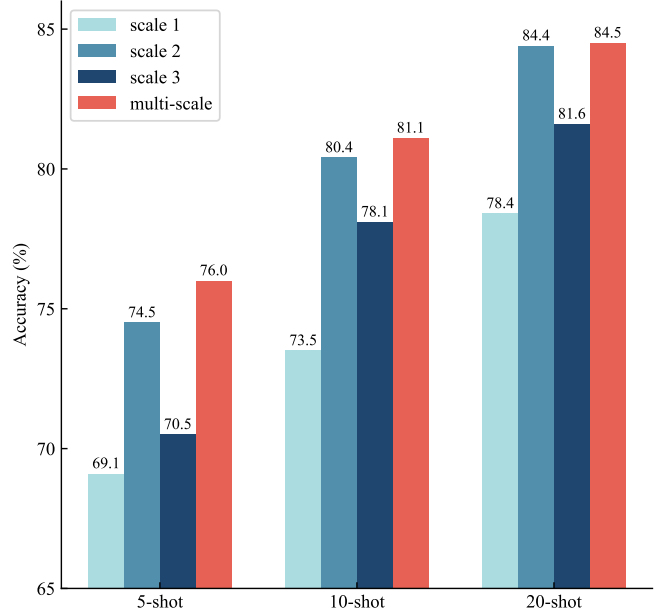


Fig. 4: Kernel settings for computing gradient by ratio. Here, the scale 1/2/3 is with r equal to 9/13/17, and the multi-scale contacts all scales. Multi-scale is more suitable than single scale for various targets in remote sensing images.

suppression. Therefore, combining features of different scales has an improvement over a single scale for various target sizes in images.

4.4 Analysis

As stated above, SARATR-X’s key points are summarized as follows: HiViT architecture avoids the loss of small target information. SSL-ImageNet & SAR use ImageNet pre-training weights to provide a good initialization for diversity perceptual capability. MGF ensures high-quality target features and suppresses speckle noise under SSL with SAR images. Benefiting the above insights, our SARATR-X can learn high-quality target features from noisy SAR remote sensing images in Table 4. Next, we analyze the diversity and scalability of SARATR-X.

Visualization. Research [85] has shown that supervised pre-training and contrastive learning only model global information in the high layer, and MIM can model both local and global information. However, we observe that this phenomenon is not only related to the methods but also to the data properties. Fig. 5 (a) shows that the ViT with MAE focuses on global information due to large SAR image scenes, which differs from MIM’s modeling properties. Therefore, HiViT has various attention ranges with its high spatial resolution and hierarchical structure in Fig. 5 (b). In addition, using ImageNet’s weight as initialization can enhance this problem in Fig. 5 (c). As for the target feature, Fig. 5 (d) displays the HOG feature enhances the noise interference, which harms feature diversity. MGF effectively extracts the shape information of the target, making the model more focused on diverse edge information in the lower layer. However, this approach removes texture and preserves edge information, which motivates the higher layers not to need to focus on texture details and diminishes the attention range in Fig. 5 (e). Therefore, we combine two-step training with MGF in Fig. 5 (f).

Scaling experiment. Although MIM is a good learner that scales with data and model resources [86], a question arises

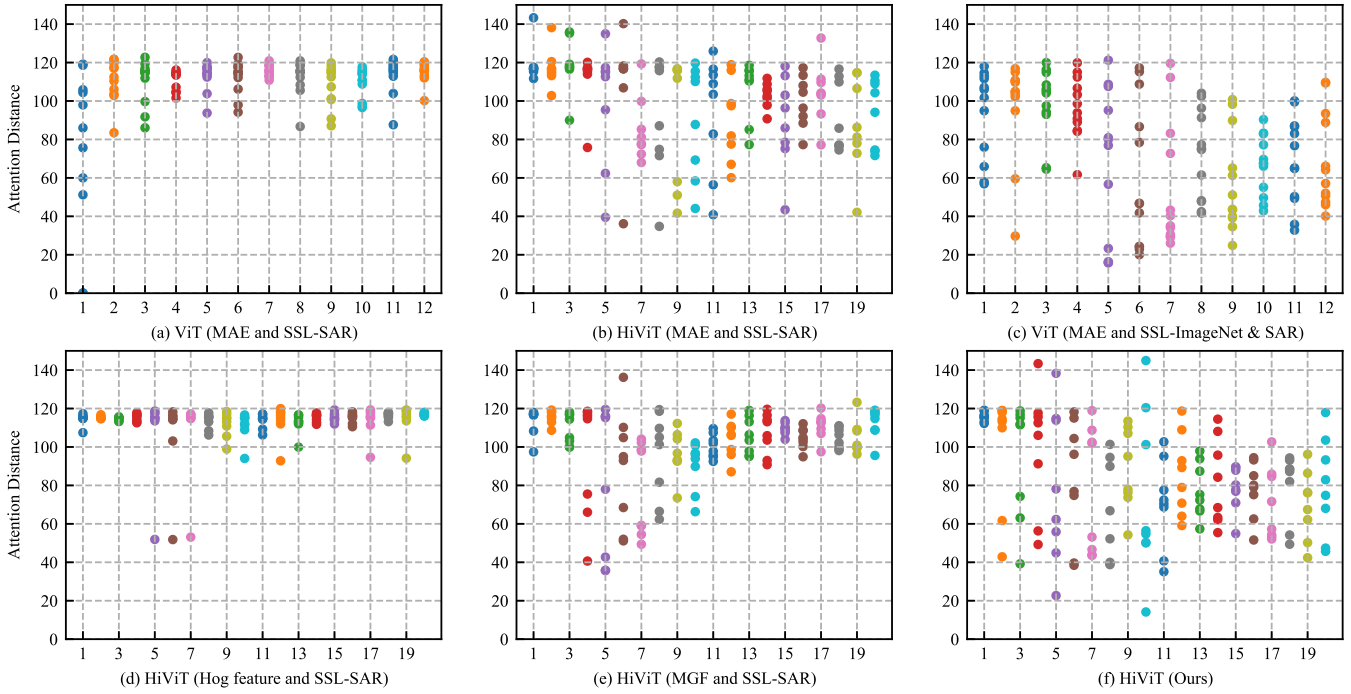


Fig. 5: Averaged attention distance in different attention heads (x-axis is the attention head *w.r.t* layer number) on SSL models. Attention distance represents the range of the receptive field. We can focus on model architectures (Fig. (a) *v.s.* Fig. (b)), initialization weights (Fig. (a) *v.s.* Fig. (c)), and SSL signals (Fig. (d) *v.s.* Fig. (e)) to ensure diverse attention ranges in SAR target recognition, such as HiViT architecture, ImageNet weights, and SAR target features.

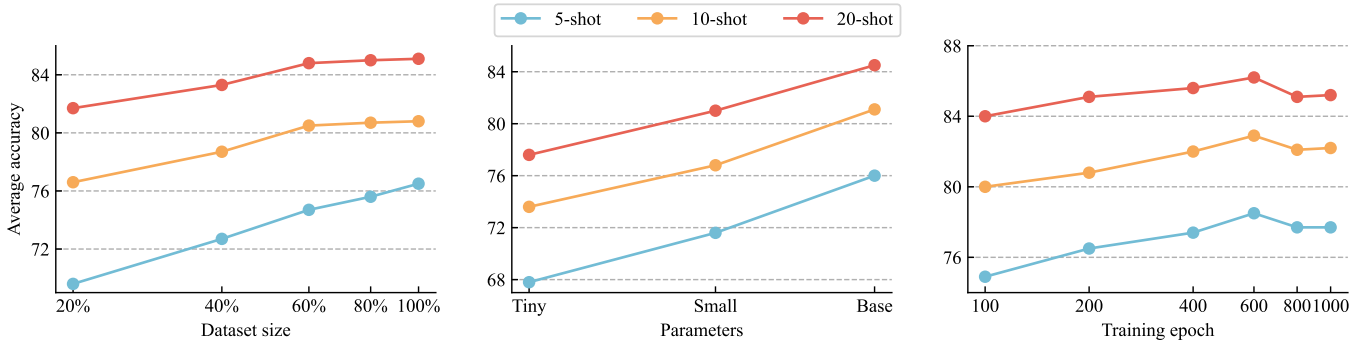


Fig. 6: Scaling ability of SARATR-X in dataset size, parameters, and training epochs with linear probing performance. Our method can benefit from these three aspects. However, it is important to note that excessive training epochs can lead to overfitting due to the dataset size and speckle noise.

as to whether our method can ensure scalability for MIM when dealing with noisy data such as SAR. Fig. 6 presents the scaling experiment from three perspectives: dataset size, parameters, and training epochs. Despite our pre-training set comprising 186,660 images, which is smaller than ImageNet-1K, we observe a significant improvement in downstream tasks’ performance with increasing data and parameters. This phenomenon indicates that the foundational model can fully unleash its potential in SAR images by extracting high-quality features as guiding signals. However, just like the study [86], when the pre-training size contains 100,000 images, the model tends to overfit during extended training epochs. Moreover, SAR image noise and low resolution can further aggravate the overfitting. However, SARATR-X outperforms our previous study, SAR-JEPA, which has overfitted at 400 epochs with 94,776 SAR images. There is a need to continue investigating how to ensure high-quality feature representation when extending the SAR foundation models.

5 LEVERAGING SARATR-X FOR RECOGNITION

We have discussed different aspects of SARATR-X, but there are many specific datasets and specialized models for SAR ATR. We thus compare our SARATR-X with other state-of-the-art methods, such as supervised learning (CSⁿNet [9] and PD [95]), semi-supervised learning (EUAPS [100]), and self-supervised learning (MSFA [43] and BIDFC [92]). We focus on SAR recognition tasks, including image classification and detection. More detailed settings³ are in appendix B.

Classification task. We study in Table 6 the performance of SARATR-X on the MSTAR [1] dataset with Standard Operating Conditions (SOCs) and Extended Operating Conditions (EOCs). We first notice that SSL (BIDFC and ours) and semi-supervised learning (EUAPS) significantly outperform other methods under small samples with additional unlabeled samples. Our results surpass the previous best by *large margins*, demonstrating the value of

3. We removed downstream tasks’ test sets from the pre-training set samples.

TABLE 6: SAR classification results on MSTAR’s SOCs and EOCs settings. SOCs are in a similar distribution and have ten types of vehicle targets. EOCs include variations for imaging conditions that belong to robustness classification and out-of-distribution problems. EOCs use depression angle, configuration, and version variations to test robustness. We find that self-supervised (BIDFC and Ours) and semi-supervised (EUAPS) methods significantly perform under the few-shot task with additional unlabeled data, demonstrating the data’s importance. Besides, our method is robust to variations in imaging parameters. The metric is accuracy \uparrow , and the detail setting follows the N -shot [94]. **Bold** indicates the best result, underline is the next best result. We provide detailed results in Appendix B.

SOCs-Standard operating conditions (10-way)				
Method	Year	1-shot	2-shot	5-shot
DKTS-N [94]	2021	49.3	58.5	72.3
ConvT [72]	2022	42.6	54.4	75.2
HDLM [74]	2022	-	-	72.4
BIDFC [92]	2022	<u>80.7</u>	<u>85.3</u>	<u>90.3</u>
CRID [73]	2023	48.3	51.0	73.3
EUAPS [100]	2023	-	-	88.7
PD [95]	2024	46.7	58.9	70.2
SARATR-X	2024	85.2 (+4.5)	91.4 (+6.1)	95.9 (+5.6)
EOCs-Depression angle variations (4-way)				
Method	Year	1-shot	2-shot	5-shot
DKTS-N [94]	2021	61.9	63.9	67.4
ConvT [72]	2022	59.6	<u>64.1</u>	68.2
CRID [73]	2023	<u>62.1</u>	62.3	<u>74.5</u>
SARATR-X	2024	93.4 (+31.3)	97.3 (+33.2)	98.9 (+24.8)
EOCs-Target configuration variations (4-way)				
Method	Year	1-shot	2-shot	5-shot
DKTS-N [94]	2021	47.3	53.6	62.2
ConvT [72]	2022	44.3	51.9	64.1
CRID [73]	2023	<u>62.8</u>	<u>65.7</u>	<u>74.1</u>
SARATR-X	2024	65.0 (+2.2)	74.0 (+8.3)	78.3 (+4.2)
EOCs-Target version variations (4-way)				
Method	Year	1-shot	2-shot	5-shot
DKTS-N [94]	2021	48.9	55.1	65.6
ConvT [72]	2022	42.3	<u>58.3</u>	<u>68.1</u>
CRID [73]	2023	<u>53.5</u>	56.2	67.2
SARATR-X	2024	65.3 (+11.8)	76.5 (+20.3)	82.8 (+15.6)

foundation models in an era of rapidly growing SAR data. In particular, our SARATR-X shows robustness to the EOC setting of imaging condition variations. This result indicates that the foundation model learns stable features and relationships from diverse imaging conditions in a large number of target samples.

Detection task. As illustrated in Table 7, we report box AP for SAR target detection with a horizontal bounding box on multi-category (SARDet-100K and OGSOD), ship (SSDD), and aircraft detection (SAR-Aircraft). SARATR-X performs better than our previous MSFA by 0.8 points on SARDet-100K. MSFA has more complex training processes and target features, which use multi-stage training between RGB and SAR images with three different target features and have a detection pre-training step. SARATR-X is more simple but more effective for SAR images. More significantly, SARATR-X outperforms or has comparable performance on various datasets compared to many specifically designed detection methods in Table 7. Of course, our study is only a preliminary exploration of SSL for SAR. More effective target features can be realized in a data-knowledge dual-driven manner by further mining the knowledge of SAR imaging mechanisms and properties. Moreover, with the larger dataset

TABLE 7: SAR detection results on SARDet-100K, OGSOD, SSDD, and SAR-Aircraft. Our proposed SARATR-X has competitive performance on various detection datasets. **Bold** indicates the best result, underline is the next best result. More detailed results are in Appendix B.

SARDet-100K (Object detection)				
Method	Year	mAP \uparrow	mAP ₅₀ \uparrow	mAP ₇₅ \uparrow
Deformable DETR [104]	2020	50.0	85.1	51.7
Swin Transformer [47]	2021	53.8	87.8	59.0
VAN [25]	2022	53.5	86.8	58.0
ConvNext [48]	2022	55.1	87.8	59.5
MSFA [43]	2024	<u>56.4</u>	<u>88.2</u>	<u>61.5</u>
SARATR-X	2024	57.3 (+0.9)	88.7 (+0.5)	62.8 (+1.3)
OGSOD (Object detection)				
Method	Year	mAP \uparrow	mAP ₅₀ \uparrow	mAP ₇₅ \uparrow
Generalized Focal [28]	2019	41.8	67.6	-
Sparse R-CNN [63]	2021	38.7	65.6	-
Object Box [91]	2022	40.1	76.6	-
YOLOv7 [75]	2022	<u>45.1</u>	<u>79.2</u>	-
SARATR-X	2024	52.0 (+6.9)	85.9 (+6.7)	51.3
SSDD (Ship detection)				
Method	Year	AP \uparrow	AP ₅₀ \uparrow	AP ₇₅ \uparrow
FBR-Net [20]	2021	-	94.1	59.1
CenterNet++ [24]	2021	-	95.1	-
CRTransSar [84]	2022	-	97.0	<u>76.2</u>
YOLO-Lite [59]	2023	-	94.4	-
FEPS-Net [3]	2023	59.9	96.0	67.5
CS ⁿ Net [9]	2023	<u>64.9</u>	<u>97.1</u>	-
SARATR-X	2024	67.5 (+2.6)	97.3 (+0.2)	83.5 (+7.3)
SAR-Aircraft (Aircraft detection)				
Method	Year	mAP \uparrow	mAP ₅₀ \uparrow	mAP ₇₅ \uparrow
Cascade R-CNN [7]	2018	-	75.7	58.9
RepPoints [89]	2019	-	72.6	53.3
SKG-Net [21]	2021	-	70.7	46.4
SA-Net [80]	2023	-	<u>77.7</u>	<u>62.8</u>
SARATR-X	2024	58.7	86.1 (+5.7)	64.7 (+3.3)

and parameters, the path of foundation models will hopefully lead to general SAR target recognition, but this goal requires researchers together.

6 CONCLUSION AND FUTURE PERSPECTIVES

In this paper, we proposed the SARATR-X for SAR ATR and systematically investigated a foundation model framework. First, a pre-training dataset was built from 14 open-source datasets, including various targets, scenes, and sensors. Then, the foundation model’s pre-training backbone, SSL methods, and downstream tasks were discussed in detail. Importantly, SARATR-X demonstrated superior performance on different target recognition datasets, demonstrating the foundation model’s potential in this field.

We believe that research on SAR foundation models, such as SARATR-X, has the potential for generalized feature representations in SAR images and accelerates towards all-day, all-weather target recognition in Earth observation. However, the research of the foundation model requires large data, which is a real problem for SAR images. SAR images are expensive and require specific imaging equipment and algorithms, and privacy and security prevent the data from opening. Therefore, we are

particularly grateful to the publishers of open-source SAR target datasets. By making SARATR-X publicly available, we aim to accelerate the progress of the foundation model in SAR target recognition by enabling researchers to use our dataset and code to design better methods or explore downstream applications.

Although this work systematically investigated a foundation model framework, several limitations and challenges require exploration in future work. The SAR images are derived from open-source SAR datasets, and the targets are mainly vehicles, ships, aircraft, oil tanks, etc. Collecting target samples from increasingly unlabelled SAR imagery could further expand the amount of data and the range of downstream applications. In addition, investigating the expert knowledge with text for multimodal interactions to describe the relationship between targets and scenes can further enhance the representation capability of the foundation model. Due to the visual variability of SAR images, textual descriptions are an effective tool for improving interpretability and comprehensibility.

In conclusion, we have verified the SARATR-X’s ability to adapt to diverse SAR target datasets, showing high performance and generalizability in classification and detection. By taking full advantage of the rapid growth of SAR images, the SSL-based foundation model opens the door to a generalized feature representation and SAR target recognition. We believe it’s time to embrace fundamental models for SAR image interpretation.

APPENDIX A IMPLEMENTATION DETAILS OF SECTION 4 EXPERIMENTS OF SARATR-X

Here are the details of the dataset and training settings.

A.1 Pre-training dataset setting

As shown in Fig. 7, we collect data from open-source datasets based on our previous research [38, 43]. Now, our pre-training dataset contains 14 open-source SAR target datasets. Here are brief descriptions of each dataset’s targets, scenes, and sensors.

AIR-SARShip [66] is a ship detection dataset based on the Chinese C-band Gaofen-3 satellite. AIR-SARShip-1.0 and AIR-SARShip-2.0 include 318 VV-polarised images with 1 and 3 m resolutions. This dataset includes harbors, islands, and different conditions of sea surfaces and covers thousands of ships.

HRSID [81] is a high-resolution dataset for ship detection and instance segmentation based on the European C-band Sentinel-1B, German X-band TerraSAR-X and TanDEM-X satellites. HRSID consists of 5,604 cropped SAR images with 0.5 to 3 m resolutions. The scene is a busy area of maritime transport, such as harbors and estuarine cities, and the annotation targets are ships of different sizes.

Sandia MiniSAR [60] is a 0.1 m resolution dataset based on a Ku-band airborne platform released by Sandia National Laboratories. The dataset contains scenes and targets such as aircraft on tarmacs, buildings in urban areas, and vehicles in desert areas but lacks official annotations.

MSAR [10, 84] is a multi-class target detection dataset based on the Chinese C-band HISEA-1 satellite in large-scale scenes. MSAR comprises 28,449 image slices with quad polarization and 1 m resolution. Scenes covered include airports, harbors, nearshore, islands, distant seas, and urban areas. The labeled target categories include aircraft, oil tanks, bridges, and ships.

MSTAR [1] is the most commonly used target classification dataset released by the Defense Advanced Research Projects

Agency, USA. Its sensor is an X-band radar with HH polarization mode and 0.3 m resolution. It contains ten categories of military vehicles with various imaging angles, target variants, and other conditions but with single grass scenes.

OGSOD [71] is a city object detection dataset collected from the Chinese C-band Gaofen-3 satellite with VV and VH polarization modes, and its resolution is 3 m. This dataset also contains optical images from Google Earth with 10 m resolution. It is annotated with static objects, including bridges, harbors, and oil tanks in urban areas.

OpenSARShip [35] is a ship slices dataset based on the European C-band Sentinel-1 satellite. Its resolution is 2.3 m to 17.4 m with VV and VH polarization. The dataset contains many ship slices from 10 busy ports. It has a diverse range of ship types but a significant category imbalance.

SADD [96] is an aircraft detection dataset collected from the German X-band TerraSAR-X satellite. Its resolution is 0.5 m to 3 m with HH polarization. The dataset contains densely parked aircraft of different sizes on airport tarmacs and runways. It has a large number of small-sized planes as well as the airport perimeter area.

SAMPLE [34] is a synthetic and measured paired fine-grained vehicle dataset released by the Air Force Research Laboratory, USA. This dataset is simulated in X-band and 0.3 m resolution. The public version provides 5,380 images of ten categories of vehicle targets at partial imaging angles.

SAR-AIRcraft [80] is a aircraft detection dataset based on the Chinese C-band Gaofen-3 satellite with 1 m resolution and single polarization. The dataset collects seven types of aircraft of different sizes from three civil airports. It can support fine-grained aircraft detection and classification studies.

SARSim [33, 51] is a fine-grained vehicle dataset created by Terma A/S, Denmark. The simulation system used for this dataset can generate X-band SAR images with resolutions ranging from 0.1m to 0.3m from CAD models. SARSim provides 21,168 vehicle samples in 7 categories (truck, car, motorbike, bus, tank, bulldozer, and pickup) and 3 scenes (grass, roads, and a mean of the two) with 7 imaging depression angles.

SAR-Ship [78] is a ship target detection dataset in complex scenes based on Chinese Gaofen-3 and European Sentinel-1 satellites. The public version of this dataset contains 39,729 images from two satellites in different imaging modes and resolutions. The dataset provides ship targets of various sizes in complex ocean scenes such as nearshore, distant seas, harbors, and islands.

SIVED [44] is a vehicle detection dataset with rotatable bounding box. It consists of vehicle slices from the MSTAR dataset [1] and vehicles in urban areas from the Sandia MiniSAR and FARAD datasets [60], and scenes include car parks, buildings, trees, roads, and others.

SSDD [97] is a commonly used SAR ship detection dataset. It is constructed based on Canadian RadarSat-2, German TerraSAR-X, and European Sentinel-1 satellites and contains different scenarios for the inshore and offshore of China and India. The dataset covers various ship sizes in different oceanic conditions with diverse clutter and noise interference.

A.2 Classification dataset for performance Test

We select three target classification datasets, including 25 fine-grained targets from vehicles, ships, aircraft, and others, to evaluate the comprehensive performance of SSL and the

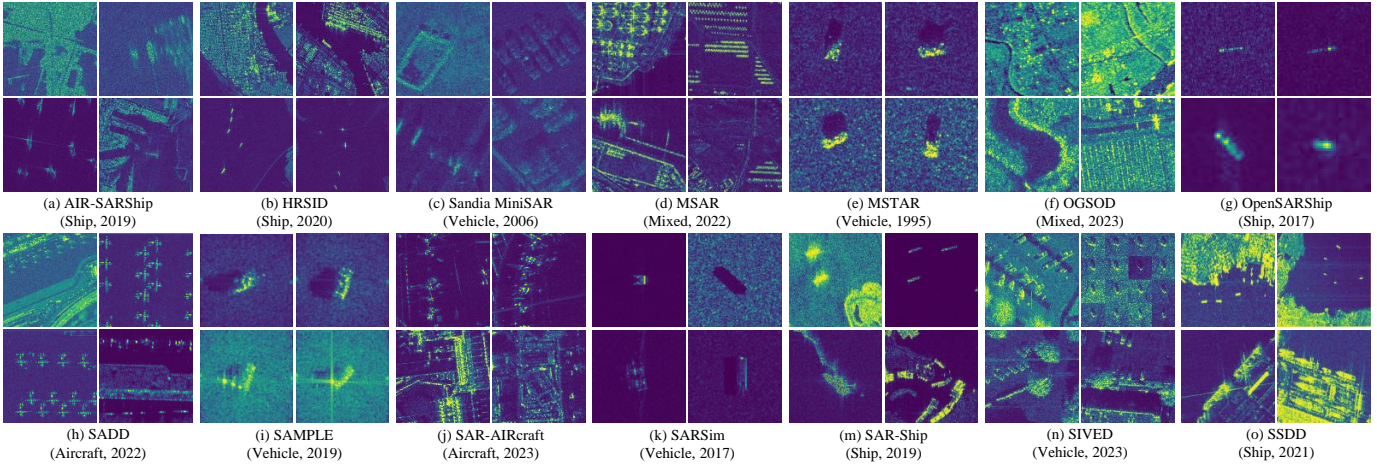


Fig. 7: Visualization of the fourteen datasets included in our pre-training. In this way, a pre-trained dataset for SAR ATR can be built with multiple targets, scenes, and sensors.

TABLE 8: Description of our SAR classification dataset, named SAR-VSA, which contains 25 fine-grained targets. # Train: Number of train samples. # Test: Number of test sample images.

Fine-grained category	# Train	# Test
anti-aircraft (ZSU234)	299	274
bulldozer (D7)	299	274
howitzer (2S1)	299	274
infantry vehicle (BMP2)	698	587
main battle tank (T62)	299	273
main battle tank (T72)	691	582
patrol car (BRDM2)	298	274
personnel carrier (BTR60)	256	195
personnel carrier (BTR70)	233	196
truck (ZIL131)	299	274
bridge	1,023	438
coastal land	707	303
land patch	1,137	487
sea clutter wave	1,378	590
sea patch	1,250	535
ship (cargo)	366	156
ship (fishing)	248	106
ship (tanker)	150	64
ship (others)	312	133
strong false alarms	299	128
aircraft (Airbus A220)	91	373
aircraft (Airbus A330)	97	415
aircraft (Comac ARJ21)	103	411
aircraft (Boeing 737)	100	428
aircraft (Boeing 787)	113	391

foundation model for SAR target recognition. The new SAR classification dataset named SAR-Target in Table 8.

MSTAR [1] is the most commonly used SAR vehicle dataset. It has many experimental setting variants, while we refer to the [40] to adopt the most commonly used ten-class classification settings, such as infantry vehicle, patrol car, personnel carrier, main battle tank, and truck.

FUSAR-Ship [64] contains 15 primary ship categories and many non-ship targets based on the Gaofen-3 satellite in scenes such as sea, land, coast, river, and island. Based on the experimental setting of [76], we have ten ocean target types, such as four fine-grained ships, bridges, and ocean scene slices.

SAR-ACD [64] contains five types of aircraft based on the

TABLE 9: Pre-training setting.

Config	Value
optimizer	AdamW [50]
base learning rate	1.5e-4
weight decay	0.05
optimizer momentum	$\beta_1, \beta_2 = 0.9, 0.95$ [12]
batch size	800
epoch	200
learning rate schedule	cosine decay [49]
warmup epoch [23]	5
augmentation	ResizedCrop, HFlip, ColorJitter

Gaofen-3 satellite in three civil airports. Since the released dataset does not separate the training and test data, we randomly select partial samples as the training set and others as the test set. Fine-grained recognition of aircraft targets is a more challenging task due to the smooth surface of the aircraft, resulting in insignificant SAR image features.

A.3 Hyperparameter settings

Here are the detailed settings of our pre-training and downstream tasks as shown in Table 9 and 10.

Pre-training. Our default pre-training setting is in Table 9, and other hyperparameters of each method use the default settings from their papers and codes. Our pre-training is applied on 8 NVIDIA RTX3090 GPUs with 200 epochs and 800 batch sizes. Compared to the training settings of MAE, we add ColorJitter (contrast = 0.5) to increase data richness. Moreover, we modify the batch size and epoch according to 8 GPUs. It is worth noting that although MAE uses the normalized pixel value to enhance the feature representation in the visible spectral images, we find that the normalized pixel value cannot be used due to the SAR image noise and prevents the training loss from decreasing properly.

Classification setting. All models use the same training settings in downstream classification tasks. Table 10 gives the default setting. Our few-shot learning setting is based on the Dssl toolbox [101, 102] and is averaged over 10 random experiments. Since we focus on the small sample case of the downstream classification task, we use the linear probing method in MAE to finetune models and avoid overfitting.

TABLE 10: Classification settings (fine-tuning and linear probing).

Config	Value
optimizer	AdamW
base learning rate	1e-3
weight decay	1e-4
optimizer momentum	$\beta_1, \beta_2 = 0.9, 0.95$
batch size	25
epoch	30
learning rate schedule	cosine decay
warmup epoch	1
warmup type	constant
warmup learning rate	1e-5

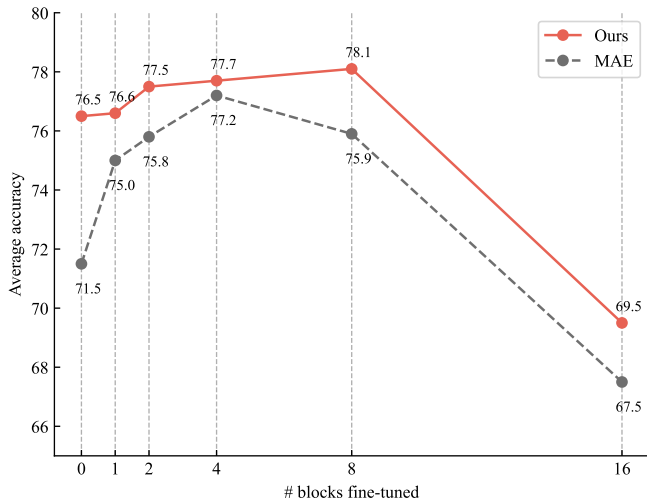


Fig. 8: Partial fine-tuning results of HiViT-B and SSL-ImageNet & SAR. Tuning 0 blocks is linear probing. With the increasing number of fine-tuned transformer blocks, our method are consistently better than MAE and experience overfitting later.

Partial fine-tuning. Fig. 8 shows why we chose linear probing for few-shot evaluation, as HiViT overfits when many blocks are fine-tuned. Experimental results show that our SAR-KGPA consistently obtains better representations than MAE, and overfitting occurs later.

APPENDIX B IMPLEMENTATION DETAILS OF SECTION 5 LEVERAGING SARATR-X FOR RECOGNITION

B.1 Dataset description

We choose MSTAR, the most commonly used dataset in SAR target classification. SOC’s are in similar image conditions, and the training set’s depression angle under SOC is 17° , while the test set is 15° . Ten categories of targets include BMP2, BRDM2, BTR60, BTR70, T62, T72, 2S1, D7, ZIL131, and ZSU234 as shown in Table 8. The EOCs setting is the imaging condition variations to test robustness. Existing methods have been saturated with different experimental settings of MSTAR [40], but few samples and depression angle variations remain challenging. We use SARDet-100K and OGSOD datasets, which have many test samples and categories, to evaluate the detection performance fully. The OGSOD comparison results are derived from the original article’s [71] single-modal approach using only SAR images. SSDD and SAR-Aircraft are ship and aircraft categories.

B.2 Hyperparameter settings

Based on our scaling experiment, we use HiViT-B with 600 epochs pre-trained on SSL-ImageNet & SAR as the foundation model for classification and detection tasks.

Classification setting is follow Table 10. The only difference is that we use partial fine-tuning for better performance, and the last 6 blocks are added to the fine-tuned.

Detection setting is follows the default setting in HiViT, and we adjust the learning rate to $5e-4$. We used the same settings for each dataset fine-tuning, see our GitHub configuration based on the mmdetection [11] framework for details.

B.3 Detailed results

We provide detail classification and detection result on Table 11 and 12. Although the proposed method outperforms existing methods in mAP, there is still scope for improvement in some refined metrics.

REFERENCES

- [1] Air Force Research Laboratory. The air force moving and stationary target recognition database. <https://www.sdms.afrl.af.mil/index.php?collection=mstar>.
- [2] Mahmoud Assran, Quentin Duval, Ishan Misra, Piotr Bojanowski, Pascal Vincent, Michael Rabbat, Yann LeCun, and Nicolas Ballas. Self-supervised learning from images with a joint-embedding predictive architecture. In *Proc. IEEE Comput. Soc. Conf. Comput. Vis. Pattern Recognit. (CVPR)*, pages 15619–15629, 2023.
- [3] Lin Bai, Cheng Yao, Zhen Ye, Dongling Xue, Xiangyuan Lin, and Meng Hui. Feature enhancement pyramid and shallow feature reconstruction network for SAR ship detection. *IEEE J. Sel. Top. Appl. Earth Obs. Remote Sens.*, 16:1042–1056, 2023.
- [4] Randall Balestriero, Mark Ibrahim, Vlad Sobal, Ari Morcos, Shashank Shekhar, Tom Goldstein, Florian Bordes, Adrien Bardes, Gregoire Mialon, Yuandong Tian, et al. A cookbook of self-supervised learning. *arXiv preprint*, 2023.
- [5] Rishi Bommasani, Drew A Hudson, Ehsan Adeli, Russ Altman, Simran Arora, Sydney von Arx, Michael S Bernstein, Jeannette Bohg, Antoine Bosselut, Emma Brunskill, et al. On the opportunities and risks of foundation models. *arXiv preprint*, 2021.
- [6] Alan C Bovik. On detecting edges in speckle imagery. *IEEE Trans. Acoust. Speech Signal Process.*, 36(10):1618–1627, 1988.
- [7] Zhaowei Cai and Nuno Vasconcelos. Cascade R-CNN: Delving into high quality object detection. In *Proc. IEEE Comput. Soc. Conf. Comput. Vis. Pattern Recognit. (CVPR)*, pages 6154–6162, 2018.
- [8] John Canny. A computational approach to edge detection. *IEEE Trans. Pattern Anal. Mach. Intell.*, (6):679–698, 1986.
- [9] Chengcheng Chen, Weiming Zeng, Xiliang Zhang, and Yuhao Zhou. CS²net: A remote sensing detection network breaking the second-order limitation of transformers with recursive convolutions. *IEEE Trans. Geosci. Remote Sens.*, 61:1–15, 2023.
- [10] Jie Chen, Zhixiang Huang, Runfan Xia, Bocai Wu, Lei Sheng, Long Sun, and Baidong Yao. Large-scale multi-class SAR image target detection dataset-1.0. <https://radars.ac.cn/web/data/getData?dataType=MSAR>, 2022.
- [11] Kai Chen, Jiaqi Wang, Jiangmiao Pang, Yuhang Cao, Yu Xiong, Xiaoxiao Li, Shuyang Sun, Wansen Feng, Ziwei Liu, Jiarui Xu, et al. MMDetection: Open mmlab detection toolbox and benchmark. *arXiv preprint*, 2019.
- [12] Kai Chen, Alec Radford, Rewon Child, Jeffrey Wu, Heewoo Jun, David Luan, and Ilya Sutskever. Generative pretraining from pixels. In *Int. Conf. Machin. Learn. (ICML)*, pages 1691–1703. PMLR, 2020.
- [13] Yezhen Cong, Samar Khanna, Chenlin Meng, Patrick Liu, Erik Rozi, Yutong He, Marshall Burke, David Lobell, and Stefano Ermon. SatMAE: Pre-training transformers for temporal and multi-spectral satellite imagery. In *Proc. Adv. Neural Inf. Process. Syst. (NeurIPS)*, volume 35, pages 197–211, 2022.
- [14] Navneet Dalal and Bill Triggs. Histograms of oriented gradients for human detection. In *Proc. IEEE Comput. Soc. Conf. Comput. Vis. Pattern Recognit. (CVPR)*, volume 1, pages 886–893. Ieee, 2005.
- [15] Mihai Datcu, Zhongling Huang, Andrei Anghel, Juanping Zhao, and Remus Căcoveanu. Explainable, physics-aware, trustworthy artificial intelligence: A paradigm shift for synthetic aperture radar. *IEEE Geosci. Remote Sens. Mag.*, 11(1):8–25, 2023.

TABLE 11: Detailed classification results on MSTAR’s SOCs and EOCs. **Bold** indicates the best result, underline is the next best result.

SOCs: Standard operating conditions (10 way)									
Method	Year	1-shot	2-shot	3-shot	4-shot	5-shot	10-shot	20-shot	25-shot
DKTS-N [94]	2021	49.3	58.5	-	-	72.3	84.6	-	96.2
ConvT [72]	2022	42.6	54.4	-	-	75.2	88.6	-	96.5
HDLM [74]	2022	-	-	-	-	72.4	88.2	95.2	-
BIDFC [92]	2022	<u>80.7</u>	<u>85.3</u>	<u>87.3</u>	<u>88.4</u>	<u>90.3</u>	-	-	-
CRID [73]	2023	48.3	51.0	-	-	73.3	87.4	96.9	97.1
EUAPS [100]	2023	-	-	-	-	88.7	98.6	99.8	-
PD [95]	2024	46.7	58.9	62.0	67.5	70.2	83.7	-	-
SARATR-X	2024	85.2	91.4	93.9	95.1	95.9	<u>97.7</u>	<u>98.1</u>	98.5
EOCs: Depression angle variations (4 way)									
Method	Year	1-shot	2-shot	3-shot	4-shot	5-shot	10-shot	20-shot	25-shot
DKTS-N [94]	2021	61.9	63.9	-	-	67.4	71.1	-	78.9
ConvT [72]	2022	59.6	<u>64.1</u>	-	-	68.2	74.8	<u>79.1</u>	-
CRID [73]	2023	<u>62.1</u>	62.3	-	-	<u>74.5</u>	<u>85.9</u>	-	<u>87.0</u>
SARATR-X	2024	93.4	97.3	98.5	98.0	98.9	99.5	99.6	99.4
EOCs: Target configuration variations (4-way)									
Method	Year	1-shot	2-shot	3-shot	4-shot	5-shot	10-shot	20-shot	25-shot
DKTS-N [94]	2021	47.3	53.6	-	-	62.2	68.4	-	74.5
ConvT [72]	2022	44.3	51.9	-	-	64.1	89.7	-	<u>91.0</u>
CRID [73]	2023	<u>62.8</u>	<u>65.7</u>	-	-	<u>74.1</u>	78.7	-	84.1
SARATR-X	2024	65.0	74.0	74.0	84.2	78.3	<u>87.0</u>	88.9	93.5
EOCs: Target version configuration variations (4-way)									
Method	Year	1-shot	2-shot	3-shot	4-shot	5-shot	10-shot	20-shot	25-shot
DKTS-N [94]	2021	48.9	55.1	-	-	65.6	70.2	-	77.0
ConvT [72]	2022	42.3	58.3	-	-	<u>68.1</u>	83.6	-	<u>92.0</u>
CRID [73]	2023	<u>53.5</u>	56.2	-	-	67.2	79.9	-	87.8
SARATR-X	2024	65.3	76.5	76.3	83.4	82.8	85.0	92.1	97.0

- [16] Flora Dellinger, Julie Delon, Yann Gousseau, Julien Michel, and Florence Tupin. SAR-SIFT: a SIFT-like algorithm for SAR images. *IEEE Trans. Geosci. Remote Sens.*, 53(1):453–466, 2014.
- [17] Zhe Dong, Yanfeng Gu, and Tianzhu Liu. Generative convnet foundation model with sparse modeling and low-frequency reconstruction for remote sensing image interpretation. *IEEE Trans. Geosci. Remote Sens.*, 2024.
- [18] Alexey Dosovitskiy, Lucas Beyer, Alexander Kolesnikov, Dirk Weissenborn, Xiaohua Zhai, Thomas Unterthiner, Mostafa Dehghani, Matthias Minderer, Georg Heigold, Sylvain Gelly, et al. An image is worth 16x16 words: Transformers for image recognition at scale. *arXiv preprint*, 2020.
- [19] Li Fei-Fei and Ranjay Krishna. Searching for computer vision north stars. *Daedalus*, 151(2):85–99, 2022.
- [20] Jiamei Fu, Xian Sun, Zhirui Wang, and Kun Fu. An anchor-free method based on feature balancing and refinement network for multiscale ship detection in SAR images. *IEEE Trans. Geosci. Remote Sens.*, 59(2):1331–1344, 2021.
- [21] Kun Fu, Jiamei Fu, Zhirui Wang, and Xian Sun. Scattering-keypoint-guided network for oriented ship detection in high-resolution and large-scale sar images. *IEEE J. Sel. Top. Appl. Earth Obs. Remote Sens.*, 14:11162–11178, 2021.
- [22] Valerio Gagliardi, Fabio Tosti, Luca Bianchini Ciampoli, Maria Libera Battagliere, Luigi D’Amato, Amir M Alani, and Andrea Benedetto. Satellite remote sensing and non-destructive testing methods for transport infrastructure monitoring: Advances, challenges and perspectives. *Remote Sens.*, 15(2):418, 2023.
- [23] Priya Goyal, Piotr Dollár, Ross Girshick, Pieter Noordhuis, Lukasz Wesolowski, Aapo Kyrola, Andrew Tulloch, Yangqing Jia, and Kaiming He. Accurate, large minibatch SGD: Training imagenet in 1 hour. *arXiv preprint*, 2017.
- [24] Haoyuan Guo, Xi Yang, Nannan Wang, and Xinbo Gao. A centernet++ model for ship detection in SAR images. *Pattern Recognit.*, 112:107787, 2021.
- [25] Meng-Hao Guo, Cheng-Ze Lu, Zheng-Ning Liu, Ming-Ming Cheng, and Shi-Min Hu. Visual attention network. *Comput. Visual Media*, 9(4):733–752, 2023.
- [26] Xin Guo, Jiangwei Lao, Bo Dang, Yingying Zhang, Lei Yu, Lixiang Ru, Liheng Zhong, Ziyuan Huang, Kang Wu, Dingxiang Hu, et al. SkySense: A multi-modal remote sensing foundation model towards universal interpretation for earth observation imagery. *arXiv preprint*, 2023.
- [27] Kaiming He, Xinlei Chen, Saining Xie, Yanghao Li, Piotr Dollár, and Ross Girshick. Masked autoencoders are scalable vision learners. In *Proc. IEEE Comput. Soc. Conf. Comput. Vis. Pattern Recognit. (CVPR)*, pages 16000–16009, 2022.
- [28] Yihui He, Chenchen Zhu, Jianren Wang, Marios Savvides, and Xiangyu Zhang. Bounding box regression with uncertainty for accurate object detection. In *Proc. IEEE Comput. Soc. Conf. Comput. Vis. Pattern Recognit. (CVPR)*, pages 2888–2897, 2019.
- [29] Zhongling Huang, Xiwen Yao, Ying Liu, Corneliu Octavian Dumitru, Mihai Datcu, and Junwei Han. Physically explainable CNN for SAR image classification. *ISPRS J. Photogramm. Remote Sens.*, 190:25–37, 2022.
- [30] Licheng Jiao, Zhongjian Huang, Xiaoqiang Lu, Xu Liu, Yuting Yang, Jiaxuan Zhao, Jinyue Zhang, Biao Hou, Shuyuan Yang, Fang Liu, Wenping Ma, Lingling Li, Xiangrong Zhang, Puhua Chen, Zhixi Feng, Xu Tang, Yuwei Guo, Dou Quan, Shuang Wang, Weibin Li, Jing Bai, Yangyang Li, Ronghua Shang, and Jie Feng. Brain-inspired remote sensing foundation models and open problems: A comprehensive survey. *IEEE J. Sel. Top. Appl. Earth Obs. Remote Sens.*, 16:10084–10120, 2023.
- [31] Odysseas Kechagias-Stamatis and Nabil Aouf. Automatic target recognition on synthetic aperture radar imagery: A survey. *IEEE Aerosp. Electron. Syst. Mag.*, 36(3):56–81, 2021.
- [32] Samar Khanna, Patrick Liu, Linqi Zhou, Chenlin Meng, Robin Rombach, Marshall Burke, David Lobell, and Stefano Ermon. DiffusionSat: A generative foundation model for satellite imagery. In *Proc. Int. Conf. Learn. Represent. (ICLR)*, 2024.
- [33] Anders Kusk, Adili Abulaitijiang, and Jorgen Dall. Synthetic SAR

TABLE 12: Detailed detection results. The metrics are mAP, mAP₅₀ (@50), mAP₇₅ (@75), mAP_{small} (@s), mAP_{medium} (@m), and mAP_{large} (@l). **Bold** indicates the best result, underline is the next best result.

SARDet-100K (Object detection)							
Method	Year	mAP	@50	@75	@s	@m	@l
Deformable DETR [104]	2020	50.0	85.1	51.7	44.0	65.1	61.2
Swin Transformer [47]	2021	53.8	87.8	59.0	49.1	64.6	60.0
VAN [25]	2022	53.5	86.8	58.0	47.3	65.5	60.6
ConvNext [48]	2022	55.1	87.8	59.5	48.9	66.9	61.1
MSFA [43]	2024	<u>56.4</u>	<u>88.2</u>	<u>61.5</u>	<u>50.5</u>	<u>66.5</u>	<u>62.5</u>
SARATR-X	2024	57.2 (+0.8)	88.5 (+0.3)	62.6 (+1.1)	51.2 (+0.7)	69.6 (+3.1)	64.7 (+2.2)
OGSOD (Object detection)							
Method	Year	mAP	@50	@75	@s	@m	@l
Generalized Focal [28]	2019	41.8	67.6	-	-	-	-
Sparse R-CNN [63]	2021	38.7	65.6	-	-	-	-
Object Box [91]	2022	40.1	76.6	-	-	-	-
YOLOv7 [75]	2022	<u>45.1</u>	<u>79.2</u>	-	-	-	-
SARATR-X	2024	51.4 (+6.3)	85.2 (+6.0)	51.7	46.8	75.3	77.1
SSDD (Ship detection)							
Method	Year	AP	@50	@75	@s	@m	@l
FBR-Net [20]	2021	-	94.1	59.1	-	-	-
CenterNet++ [24]	2021	-	95.1	-	-	-	-
CRTransSar [84]	2022	-	97.0	<u>76.2</u>	-	-	-
YOLO-Lite [59]	2023	-	94.4	-	-	-	-
FEPS-Net [3]	2023	59.9	96.0	67.5	<u>55.1</u>	68.2	70.6
CS ⁿ Net [9]	2023	<u>64.9</u>	<u>97.1</u>	-	-	-	-
SARATR-X	2024	67.4 (+2.5)	97.3 (+0.2)	83.1 (+6.9)	68.1 (+13.0)	<u>66.1 (-2.1)</u>	<u>60.5 (-10.1)</u>
SAR-Aircraft (Aircraft detection)							
Method	Year	AP	@50	@75	@s	@m	@l
Cascade R-CNN [7]	2018	-	75.7	58.9	-	-	-
RepPoints [89]	2019	-	72.6	53.3	-	-	-
SKG-Net [21]	2021	-	70.7	46.4	-	-	-
SA-Net [80]	2023	-	<u>77.7</u>	<u>62.8</u>	-	-	-
SARATR-X	2024	58.7	86.1 (+5.7)	64.7 (+3.3)	20.0	57.2	49.7

- image generation using sensor, terrain and target models. In *Proc. Eur. Conf. Synth. Aperture Radar, EUSAR 2016*, pages 1–5. VDE, 2016.
- [34] Benjamin Lewis, Theresa Scarnati, Elizabeth Sudkamp, John Nehrbass, Stephen Rosencrantz, and Edmund Zelnio. A SAR dataset for ATR development: the synthetic and measured paired labeled experiment (SAMPLE). In *Proc. SPIE Conf. Algorithms SAR Imagery*, volume 10987, pages 39–54, 2019.
- [35] Boying Li, Bin Liu, Lanqing Huang, Weiwei Guo, Zenghui Zhang, and Wenxian Yu. OpenSARShip 2.0: A large-volume dataset for deeper interpretation of ship targets in Sentinel-1 imagery. In *Proc. SAR Big Data Era: Models Methods Appl. (BIGSAR DATA)*, pages 1–5, 2017.
- [36] Jianwei Li, Congan Xu, Hang Su, Long Gao, and Taoyang Wang. Deep learning for SAR ship detection: Past, present and future. *Remote Sens.*, 14(11):2712, 2022.
- [37] Jianwei Li, Zhenao Yu, Lu Yu, Pu Cheng, Jie Chen, and Cheng Chi. A comprehensive survey on SAR ATR in deep-learning era. *Remote Sens.*, 15(5):1454, 2023.
- [38] Weijie Li, Yang Wei, Tianpeng Liu, Yuenan Hou, Yongxiang Liu, and Li Liu. Predicting gradient is better: Exploring self-supervised learning for SAR ATR with a joint-embedding predictive architecture. *arXiv preprint*, 2024.
- [39] Weijie Li, Wei Yang, Li Liu, Wenpeng Zhang, and Yongxiang Liu. Discovering and explaining the noncausality of deep learning in SAR ATR. *IEEE Geosci. Remote Sens. Lett.*, 20:1–5, 2023.
- [40] Weijie Li, Wei Yang, Wenpeng Zhang, Tianpeng Liu, Yongxiang Liu, and Li Liu. Hierarchical disentanglement-alignment network for robust SAR vehicle recognition. *IEEE J. Sel. Top. Appl. Earth Obs. Remote Sens.*, 16:9661–9679, 2023.
- [41] Xiang Li, Congcong Wen, Yuan Hu, Zhenghang Yuan, and Xiao Xiang Zhu. Vision-language models in remote sensing: Current progress and future trends. *IEEE Geosci. Remote Sens. Mag.*, pages 2–36, 2024.
- [42] Yuxuan Li, Qibin Hou, Zhaohui Zheng, Ming-Ming Cheng, Jian Yang, and Xiang Li. Large selective kernel network for remote sensing object detection. In *Proc. IEEE Int. Conf. Comput. Vis. (ICCV)*, pages 16794–16805, October 2023.
- [43] Yuxuan Li, Xiang Li, Weijie Li, Qibin Hou, Li Liu, Ming-Ming Cheng, and Jian Yang. SARDet-100K: Towards open-source benchmark and toolkit for large-scale SAR object detection. *arXiv preprint*, 2024.
- [44] Xin Lin, Bo Zhang, Fan Wu, Chao Wang, Yali Yang, and Huiqin Chen. SIVED: A SAR image dataset for vehicle detection based on rotatable bounding box. *Remote Sens.*, 15(11):2825, 2023.
- [45] Xiao Liu, Fanjin Zhang, Zhenyu Hou, Li Mian, Zhaoyu Wang, Jing Zhang, and Jie Tang. Self-supervised learning: Generative or contrastive. *IEEE Trans. Knowl. Data Eng.*, 35(1):857–876, 2021.
- [46] Yuan Liu, Songyang Zhang, Jiacheng Chen, Kai Chen, and Dahua Lin. PixMIM: Rethinking pixel reconstruction in masked image modeling. *arXiv preprint*, 2023.
- [47] Ze Liu, Yutong Lin, Yue Cao, Han Hu, Yixuan Wei, Zheng Zhang, Stephen Lin, and Baining Guo. Swin transformer: Hierarchical vision transformer using shifted windows. In *Proc. IEEE Comput. Soc. Conf. Comput. Vis. Pattern Recognit. (CVPR)*, pages 10012–10022, 2021.
- [48] Zhuang Liu, Hanzhi Mao, Chao-Yuan Wu, Christoph FeChtenhofer, Trevor Darrell, and Saining Xie. A ConvNet for the 2020s. In *Proc. IEEE Comput. Soc. Conf. Comput. Vis. Pattern Recognit. (CVPR)*, pages 11976–11986, 2022.
- [49] Ilya Loshchilov and Frank Hutter. SGDR: Stochastic gradient descent with warm restarts. 2017.
- [50] Ilya Loshchilov and Frank Hutter. Decoupled weight decay regularization. 2019.
- [51] David Malmgren-Hansen, Anders Kusk, Jørgen Dall, Allan Aasbjerg Nielsen, Rasmus Engholm, and Henning Skriver. Improving SAR automatic target recognition models with transfer learning from

- simulated data. *IEEE Geosci. Remote Sens. Lett.*, 14(9):1484–1488, 2017.
- [52] Matías Mendieta, Boran Han, Xingjian Shi, Yi Zhu, and Chen Chen. Towards geospatial foundation models via continual pretraining. In *Proc. IEEE Comput. Soc. Conf. Comput. Vis. Pattern Recognit. (CVPR)*, pages 16806–16816, 2023.
- [53] Alberto Moreira, Pau Prats-Iraola, Marwan Younis, Gerhard Krieger, Irena Hajnsek, and Konstantinos P Papatthanassiou. A tutorial on synthetic aperture radar. *IEEE Geosci. Remote Sens. Mag.*, 1(1):6–43, 2013.
- [54] Dilxat Muhtar, Zhenshi Li, Feng Gu, Xueliang Zhang, and Pengfeng Xiao. LHRs-Bot: Empowering remote sensing with vgi-enhanced large multimodal language model. *arXiv preprint*, 2024.
- [55] Dilxat Muhtar, Xueliang Zhang, Pengfeng Xiao, Zhenshi Li, and Feng Gu. Cmid: A unified self-supervised learning framework for remote sensing image understanding. *IEEE Trans. Geosci. Remote Sens.*, 2023.
- [56] Hao Pei, Mingjie Su, Gang Xu, Mengdao Xing, and Wei Hong. Self-supervised feature representation for SAR image target classification using contrastive learning. *IEEE J. Sel. Top. Appl. Earth Obs. Remote Sens.*, 16:9246–9258, 2023.
- [57] Bowen Peng, Bo Peng, Jie Zhou, Jianyue Xie, and Li Liu. Scattering model guided adversarial examples for SAR target recognition: Attack and defense. *IEEE Trans. Geosci. Remote Sens.*, 60:1–17, 2022.
- [58] Colorado J Reed, Ritwik Gupta, Shufan Li, Sarah Brockman, Christopher Funk, Brian Clipp, Kurt Keutzer, Salvatore Candido, Matt Uyttendaele, and Trevor Darrell. Scale-MAE: A scale-aware masked autoencoder for multiscale geospatial representation learning. In *Proc. IEEE Int. Conf. Comput. Vis. (ICCV)*, pages 4065–4076, 2023.
- [59] Xiaozhen Ren, Yanwen Bai, Gang Liu, and Ping Zhang. YOLO-Lite: An efficient lightweight network for SAR ship detection. *Remote Sens.*, 15(15):3771, 2023.
- [60] Sandia National Laboratories. Complex SAR data. <https://www.sandia.gov/radar/complex-data/index.html>.
- [61] Shengli Song, Bin Xu, and Jian Yang. SAR target recognition via supervised discriminative dictionary learning and sparse representation of the SAR-HOG feature. *Remote Sens.*, 8(8):683, 2016.
- [62] Guang-Cai Sun, Yanbin Liu, Jixiang Xiang, Wenkang Liu, Mengdao Xing, and Jianlai Chen. Spaceborne synthetic aperture radar imaging algorithms: An overview. *IEEE Geosci. Remote Sens. Mag.*, 10(1):161–184, 2021.
- [63] Peize Sun, Rufeng Zhang, Yi Jiang, Tao Kong, Chenfeng Xu, Wei Zhan, Masayoshi Tomizuka, Lei Li, Zehuan Yuan, Changhu Wang, et al. Sparse R-CNN: End-to-end object detection with learnable proposals. In *Proc. IEEE Comput. Soc. Conf. Comput. Vis. Pattern Recognit. (CVPR)*, pages 14454–14463, 2021.
- [64] Xian Sun, Yixuan Lv, Zhirui Wang, and Kun Fu. SCAN: Scattering characteristics analysis network for few-shot aircraft classification in high-resolution SAR images. *IEEE Trans. Geosci. Remote Sens.*, 60:1–17, 2022.
- [65] Xian Sun, Peijin Wang, Wanxuan Lu, Zicong Zhu, Xiaonan Lu, Qibin He, Junxi Li, Xuee Rong, Zhujun Yang, Hao Chang, Qinglin He, Guang Yang, Ruiping Wang, Jiwen Lu, and Kun Fu. RingMo: A remote sensing foundation model with masked image modeling. *IEEE Trans. Geosci. Remote Sens.*, 61:1–22, 2023.
- [66] Xian Sun, Zhirui Wang, Yuanrui Sun, Wenhui Diao, Yue Zhang, and Kun Fu. AIR-SARShip-1.0: High-resolution SAR ship detection dataset. *J. Radars*, 8(6):852–862, 2019.
- [67] Chao Tao, Ji Qi, Guo Zhang, Qing Zhu, Weipeng Lu, and Haifeng Li. TOV: The original vision model for optical remote sensing image understanding via self-supervised learning. *IEEE J. Sel. Top. Appl. Earth Obs. Remote Sens.*, 16:4916–4930, 2023.
- [68] Ridha Touzi, Armand Lopes, and Pierre Bousquet. A statistical and geometrical edge detector for SAR images. *IEEE Trans. Geosci. Remote Sens.*, 26(6):764–773, 1988.
- [69] Arsenios Tsokas, Maciej Rysz, Panos M Pardalos, and Kathleen Dipple. SAR data applications in earth observation: An overview. *Expert Syst. Appl.*, 205:117342, 2022.
- [70] Paul Viola and Michael Jones. Rapid object detection using a boosted cascade of simple features. In *Proc. IEEE Comput. Soc. Conf. Comput. Vis. Pattern Recognit. (CVPR)*, volume 1, pages I–I. Ieee, 2001.
- [71] Chao Wang, Rui Ruan, Zhicheng Zhao, Chenglong Li, and Jin Tang. Category-oriented localization distillation for SAR object detection and a unified benchmark. *IEEE Trans. Geosci. Remote Sens.*, 61:1–14, 2023.
- [72] Chenwei Wang, Yulin Huang, Xiaoyu Liu, Jifang Pei, Yin Zhang, and Jianyu Yang. Global in local: A convolutional transformer for SAR ATR FSL. *IEEE Geosci. Remote Sens. Lett.*, 19:1–5, 2022.
- [73] Chenwei Wang, Siyi Luo, Jifang Pei, Yulin Huang, Yin Zhang, and Jianyu Yang. Crucial feature capture and discrimination for limited training data SAR ATR. *ISPRS J. Photogramm. Remote Sens.*, 204:291–305, 2023.
- [74] Chenwei Wang, Jifang Pei, Jianyu Yang, Xiaoyu Liu, Yulin Huang, and Deqing Mao. Recognition in label and discrimination in feature: A hierarchically designed lightweight method for limited data in SAR ATR. *IEEE Trans. Geosci. Remote Sens.*, 60:1–13, 2022.
- [75] Chien-Yao Wang, Alexey Bochkovskiy, and Hong-Yuan Mark Liao. YOLOv7: Trainable bag-of-freebies sets new state-of-the-art for real-time object detectors. In *Proc. IEEE Comput. Soc. Conf. Comput. Vis. Pattern Recognit. (CVPR)*, pages 7464–7475, 2023.
- [76] Di Wang, Yongping Song, Junnan Huang, Daoxiang An, and Leping Chen. SAR target classification based on multiscale attention super-class network. *IEEE J. Sel. Top. Appl. Earth Obs. Remote Sens.*, 15:9004–9019, 2022.
- [77] Di Wang, Qiming Zhang, Yufei Xu, Jing Zhang, Bo Du, Dacheng Tao, and Liangpei Zhang. Advancing plain vision transformer toward remote sensing foundation model. *IEEE Trans. Geosci. Remote Sens.*, 61:1–15, 2022.
- [78] Ke Wang, Gong Zhang, and Henry Leung. SAR target recognition based on cross-domain and cross-task transfer learning. *IEEE Access*, 7:153391–153399, 2019.
- [79] Yi Wang, Hugo Hernández Hernández, Conrad M Albrecht, and Xiao Xiang Zhu. Feature guided masked autoencoder for self-supervised learning in remote sensing. *arXiv preprint*, 2023.
- [80] Zhirui Wang, Yuzhuo Kang, Xuan Zeng, Yuelei Wang, Ting Zhang, and Xian Sun. SAR-AIRCRAFT-1.0: High-resolution SAR aircraft detection and recognition dataset (in chinese). *J. Radars*, 12(4):906–922, 2023.
- [81] Shunjun Wei, Xiangfeng Zeng, Qizhe Qu, Mou Wang, Hao Su, and Jun Shi. HRSID: A high-resolution SAR images dataset for ship detection and instance segmentation. *IEEE Access*, 8:120234–120254, 2020.
- [82] ZaiDao Wen, ZhunGa Liu, Shuai Zhang, and Quan Pan. Rotation awareness based self-supervised learning for SAR target recognition with limited training samples. *IEEE Trans. Image Process.*, 30:7266–7279, 2021.
- [83] Sanghyun Woo, Shoubhik Debnath, Ronghang Hu, Xinlei Chen, Zhuang Liu, In So Kweon, and Saining Xie. ConvNeXt V2: Co-designing and scaling ConvNets with masked autoencoders. In *Proc. IEEE Comput. Soc. Conf. Comput. Vis. Pattern Recognit. (CVPR)*, pages 16133–16142, 2023.
- [84] Runfan Xia, Jie Chen, Zhixiang Huang, Huiyao Wan, Bocai Wu, Long Sun, Baidong Yao, Haibing Xiang, and Mengdao Xing. CRTransSar: A visual transformer based on contextual joint representation learning for SAR ship detection. *Remote Sens.*, 14(6):1488, 2022.
- [85] Zhenda Xie, Zigang Geng, Jingcheng Hu, Zheng Zhang, Han Hu, and Yue Cao. Revealing the dark secrets of masked image modeling. In *Proc. IEEE Comput. Soc. Conf. Comput. Vis. Pattern Recognit. (CVPR)*, pages 14475–14485, 2023.
- [86] Zhenda Xie, Zheng Zhang, Yue Cao, Yutong Lin, Yixuan Wei, Qi Dai, and Han Hu. On data scaling in masked image modeling. In *Proc. IEEE Comput. Soc. Conf. Comput. Vis. Pattern Recognit. (CVPR)*, pages 10365–10374, 2023.
- [87] Zhitong Xiong, Yi Wang, Fahong Zhang, and Xiao Xiang Zhu. One for All: Toward unified foundation models for earth vision. *arXiv preprint*, 2024.
- [88] Yanjie Xu, Hao Sun, Jin Chen, Lin Lei, Kefeng Ji, and Gangyao Kuang. Adversarial self-supervised learning for robust SAR target recognition. *Remote Sens.*, 13(20):4158, 2021.
- [89] Ze Yang, Shaohui Liu, Han Hu, Liwei Wang, and Stephen Lin. RepPoints: Point set representation for object detection. In *Proc. IEEE Int. Conf. Comput. Vis. (ICCV)*, pages 9657–9666, 2019.
- [90] Fanglong Yao, Wanxuan Lu, Heming Yang, Liangyu Xu, Chenglong Liu, Leyi Hu, Hongfeng Yu, Nayu Liu, Chubo Deng, Deke Tang, et al. RingMo-Sense: Remote sensing foundation model for spatiotemporal prediction via spatiotemporal evolution disentangling. *IEEE Trans. Geosci. Remote Sens.*, 2023.
- [91] Mohsen Zand, Ali Etemad, and Michael Greenspan. ObjectBox: From centers to boxes for anchor-free object detection. In *Proc. Europ. Conf. Comp. Visi. (ECCV)*, pages 390–406. Springer, 2022.
- [92] Yikui Zhai, Wenlve Zhou, Bing Sun, Jingwen Li, Qirui Ke, Zilu Ying, Junying Gan, Chaoyun Mai, Ruggero Donida Labati, Vincenzo Piuri, and Fabio Scotti. Weakly contrastive learning via batch instance discrimination and feature clustering for small sample SAR ATR. *IEEE Trans. Geosci. Remote Sens.*, 60:1–17, 2022.
- [93] Yang Zhan, Zhitong Xiong, and Yuan Yuan. SkyEyeGPT: Unifying remote sensing vision-language tasks via instruction tuning with large language model. *arXiv preprint*, 2024.
- [94] Linbin Zhang, Xiangguang Leng, Sijia Feng, Xiaojie Ma, Kefeng Ji, Gangyao Kuang, and Li Liu. Domain knowledge powered two-stream deep network for few-shot SAR vehicle recognition. *IEEE Trans. Geosci. Remote Sens.*, 60:1–15, 2021.
- [95] Linbin Zhang, Xiangguang Leng, Sijia Feng, Xiaojie Ma, Kefeng Ji,

- Gangyao Kuang, and Li Liu. Optimal azimuth angle selection for limited SAR vehicle target recognition. *ISPRS J. Photogramm. Remote Sens.*, 128:103707, 2024.
- [96] Peng Zhang, Hao Xu, Tian Tian, Peng Gao, Linfeng Li, Tianming Zhao, Nan Zhang, and Jinwen Tian. SEFEPNet: Scale expansion and feature enhancement pyramid network for SAR aircraft detection with small sample dataset. *IEEE J. Sel. Top. Appl. Earth Obs. Remote Sens.*, 15:3365–3375, 2022.
- [97] Tianwen Zhang, Xiaoling Zhang, Jianwei Li, Xiaowo Xu, Baoyou Wang, Xu Zhan, Yanqin Xu, Xiao Ke, Tianjiao Zeng, Hao Su, et al. SAR ship detection dataset (SSDD): Official release and comprehensive data analysis. *Remote Sens.*, 13(18):3690, 2021.
- [98] Wei Zhang, Miaoxin Cai, Tong Zhang, Yin Zhuang, and Xuerui Mao. EarthGPT: A universal multi-modal large language model for multi-sensor image comprehension in remote sensing domain. *arXiv preprint*, 2024.
- [99] Xiaosong Zhang, Yunjie Tian, Lingxi Xie, Wei Huang, Qi Dai, Qixiang Ye, and Qi Tian. HiVit: A simpler and more efficient design of hierarchical vision transformer. In *Proc. Int. Conf. Learn. Represent. (ICLR)*, 2023.
- [100] Xinzheng Zhang, Yuqing Luo, and Liping Hu. Semi-supervised SAR ATR via epoch- and uncertainty-aware pseudo-label exploitation. *IEEE Trans. Geosci. Remote Sens.*, 61:1–15, 2023.
- [101] Kaiyang Zhou, Ziwei Liu, Yu Qiao, Tao Xiang, and Chen Change Loy. Domain generalization: A survey. *IEEE Trans. Pattern Anal. Mach. Intell.*, 45(4):4396–4415, 2023.
- [102] Kaiyang Zhou, Yongxin Yang, Yu Qiao, and Tao Xiang. Domain adaptive ensemble learning. *IEEE Trans. Image Process.*, 30:8008–8018, 2021.
- [103] Yukun Zhou, Mark A Chia, Siegfried K Wagner, Murat S Ayhan, Dominic J Williamson, Robbert R Struyven, Timing Liu, Moucheng Xu, Mateo G Lozano, Peter Woodward-Court, et al. A foundation model for generalizable disease detection from retinal images. *Nature*, 622(7981):156–163, 2023.
- [104] Xizhou Zhu, Weijie Su, Lewei Lu, Bin Li, Xiaogang Wang, and Jifeng Dai. Deformable DETR: Deformable transformers for end-to-end object detection. *arXiv preprint*, 2020.